


MOTOROLA


Certificate Number: 2518.01

FCC ID: ABZ99FT4080
DECLARATION OF COMPLIANCE MPE ASSESSMENT

Networks & Enterprise
EME Test Laboratory
8000 West Sunrise Blvd
Fort Lauderdale, FL. 33322

Date of Report: November 30, 2006
Report Revision: Rev. O
Report ID: FCC MPE rpt_XPR UHF Rev O_061130_SR4526,
4527, 4528

Responsible Engineer: Stephen Whalen (SR Staff EME Eng.)
Date/s Tested: 10/30/2006, 11/03/2006
Manufacturer/Location: Motorola / Penang
Date submitted for test: 10/23/2006
DUT Description: UHF Range 1, 25-40W, w/ GPS and a mini-U connector.
Test TX mode(s): CW
Max. Power output: 48W, 50% Duty Cycle
TX Frequency Bands: 403-470MHz
Signaling type: FM and TDMA 1:2
Model(s) Tested: PMUE2345A
Model(s) Certified: PMUE2345A
Serial Number(s): M01DLOGK
Classification: Occupational Controlled (Operator); General Population/Uncontrolled (Passengers/Bystanders)
Rule Part(s): 2.1091 (d)

**Approved Accessories:**

Antenna(s):
PMAE4032A (406-420MHz 5/8 wave roof mount antenna; 3.5dBd gain, GPS base included),
PMAE4033A (450-470MHz 5/8 wave roof mount antenna; 3.5dBd gain, GPS base included),
PMAE4034A (450-470MHz 5/8 wave roof mount antenna; 5.0dBd gain, GPS base included)

Final RF Exposure Results:
Mobile max calculated 1-g Avg. S.A.R.: 0.251mW/g

Based on the information and the testing results provided herein, the undersigned certifies that when used as stated in the operating instructions supplied, said product complies with the national and international reference standards and guidelines listed in section 3.0 of this report. This report shall not be reproduced without written approval from an officially designated representative of the Motorola EME Laboratory.

Signature on file

Deanna Zakharia NE EME Lab Senior Resource Manager,
Laboratory Director,

Approval Date: 11/30/2006

Certification Date:

Certification No.:

TABLE OF CONTENTS

Part I

1.0	Product and System Description
2.0	Additional Options and Accessories
3.0	Measurement and Limit Standards
4.0	Data Collection Consideration
5.0	Measurement System Uncertainty Levels
6.0	Method of Measurement
6.1	EME measurements made with trunk mounted antenna(s)
6.1.1	External vehicle EME measurement
6.1.2	Internal vehicle EME measurement
6.2	EME measurements made with roof mounted antenna
6.2.1	External vehicle EME measurements
6.2.2	Internal vehicle EME measurement
7.0	Test Site
8.0	Measurement System/Equipment
9.0	Test Unit Description
10.0	Test Set-Up Description
11.0	Test Results Summary
12.0	Conclusion

APPENDIX A: Illustration of Antenna Location and Test Distances

APPENDIX B: Meter/Probe Calibration Certificates

APPENDIX C: Photos of Assessed Antennas

APPENDIX D: Detailed MPE Measurement Data

Part II

Computational EME Compliance Assessment

REVISION HISTORY

Date	Revision	Comments
11/30/06	O	This report is an addendum to the original report (dated 06/07/06) to include data for the newly offered antennas.

1.0 Product and System Description

FCC ID: ABZ99FT4080, model PMUE2345A is a mobile transceiver that utilizes both analog and digital two-way radio communications and also includes GPS capability. The modulation scheme used for analog is narrowband Frequency Modulation (FM). The modulation scheme used for digital is 4 Level Frequency Shift Keying (4FSK) and Time Division Multiple Access (TDMA). TDMA is used to allocate portions of the RF signal by dividing time into two slots. Transmission from a unit or base station is accommodated in time-slot lengths of 30 milliseconds and frame lengths of 60 milliseconds.

The intended use of the radio is Push-To-Talk (PTT) while the device is properly installed in a vehicle with an external antenna mounted at the center of the roof or trunk.

This device will be marketed to and used by employees solely for work-related operations, such as public safety agencies, e.g. police, fire and emergency medical. User training is the responsibility of these agencies which can be expected to employ the usage instructions, safety information and operational cautions set forth in the user's manual, instructional sessions or other means.

Accordingly this product is classified as Occupational/Controlled Exposure. However, In accordance with FCC requirements, the passengers inside the vehicle and the bystanders external to the vehicle are evaluated to the General Population/Uncontrolled Exposure Limits.

(Note that "By-standers" as used herein mean people other than operator)

2.0 Additional Options and Accessories:

NA

3.0 Measurement and Limit Standards

Measurements were performed according to the recommended guidelines in IEEE/ANSI C95.3-2002 and compared to FCC Limits Per 47 CFR 2.1091 (d) for General Population/Uncontrolled RF Exposure.

For test frequencies ranging from 406-470MHz the MPE (Maximum Permissible Exposure) limit to electromagnetic energy in equivalent plane wave free-space power density is 0.27 – 0.31mW/cm² and calculated using the formula f/1500.

4.0 Data Collection Consideration

Power density testing was performed with DUT installed in a 1991 Ford Taurus (4-door). Measurement data was taken with the vehicles' electrical system powered by an equivalent source equal to the car running at idle and the vehicle battery measuring 13.8 volts.

5.0 Measurement System Uncertainty Levels

The information below presents an estimate of the possible errors that are associated with the measurement system.

Uncertainty Budget for Near Field Probe Measurements

	Tol. (\pm %)	Prob. . Dist.	Divisor	u_i (\pm %)
Measurement System				
Survey Meter Calibration	3.0	N	1.00	3.0
Repeatability Accuracy	7.0	N	1.00	7.0
Combined Standard Uncertainty		RSS		7.6
Expanded Uncertainty		$k=2$		15

6.0 Method of Measurement

6.1 EME measurements made with trunk mounted antenna(s)

(For reference, see Illustration of antenna location and test distances in appendix A)

6.1.1 External vehicle EME measurement

(Antenna mounted at trunk center)

MPE measurements for by-stander conditions are determined by taking the average of (10) measurements in a 2m vertical line for each of the (3) test locations indicated in appendix A with 20cm increments at the test distance of 90cm from the antenna under test. The measurement probe sensor is rotated 180° at each of the ten incremental measurements to ensure the highest result is captured. These measurements are representative of persons other than the operator standing next to the vehicle.

Each of the offered antennas mounted at the center of the trunk were assessed at the rear of the vehicle while maintaining a twenty (20) centimeter separation distance between the probe sensor and vehicle body. The worst case frequency per antenna was then tested at a 45° radial at the corner of the trunk, and 90° radial at the side of the trunk.

For the current test vehicle, the antenna to probe sensor separation distance is 90cm (directly behind vehicle), 99.5 cm (45 degree radial) and 104 cm (90 degree radial).

Note: The distance from the trunk-mounted antenna to the edge of the vehicle is 26cm and the distance from the edge of the vehicle's trunk to the MPE vertical line assessment is 64cm (trunk to edge of bumper is 10cm). The radial distance measured at 45° from corner of trunk to vertical test line is 99.5cm. The radial distance measured at 90° from the side of the trunk is 104cm.

6.1.2 Internal vehicle EME measurement (Antenna mounted at trunk center)

While rotating survey meter probe through 180 degrees to ensure that the highest level is found, scans were performed inside of the vehicle, at both front and back seating areas, across the TX band to ascertain the highest level at the head. After the highest level is found, scans were performed vertically making two (2) additional measurements within an area approximately 40cm wide (representing the width of a person) so as to have a total of three (3) measured points, indicated below, that are averaged.

- a) Head area
- b) Chest area
- c) Lower Trunk area

6.2 EME measurements made with roof mounted antenna(s)

(For reference, see Illustration of antenna location and test distances in appendix A).

6.2.1 External vehicle EME measurement (Antenna mounted at roof center)

MPE measurements for by-stander conditions are determined by taking the average of (10) measurements in a 2m vertical line for the test location indicated in appendix A with 20cm increments at the test distance of 90cm from the antenna under test. The measurement probe sensor is rotated 180° at each of the ten incremental measurements to ensure the highest result is captured. These measurements are representative of persons other than the operator standing next to the vehicle.

Note: Actual test distance was 110cm (60cm from antenna to roof edge; 30cm from roof edge to edge of car door; 20cm vertical test line to car door); this is the closest distance that can be achieved to an antenna mounted to the center of the vehicle used for MPE compliance assessment.

6.2.2 Internal vehicle EME measurement (Antenna mounted at roof center)

While rotating survey meter probe through 180 degrees to ensure that the highest level is found, scans were performed inside of the vehicle, both at the front and back seating areas, across the TX band to ascertain the highest level in each location. After the highest level is found, two (2) additional measurements were performed vertically within an area approximately 40cm wide (representing the width of a person) so as to have a total of three (3) measured points as indicated below that are averaged.

- a) Head area
- b) Chest area
- c) Lower Trunk area

7.0 Test Site

The test site is the Motorola open area test site located at 8000 W. Sunrise Blvd., Plantation, FL. 33322.

8.0 Measurement System/Equipment

Equipment Type	Model #	SN	Calibration Due Date
Automobile	1991 Ford Taurus, 4-Door		
Survey Meter	NARDA Model 8718	01122	4/20/07
Probe - E-Field (Electric Field)	NARDA Model 8722B	12023	4/20/07

9.0 Test Unit Description

Power density measurements were performed on PMUE2345A with serial numbers M01DLOGK. The tested frequencies and associated power outputs are presented below.

Frequency (MHz)	Po (W)
406	47.7
413	47.1
416.5	47.2
450	47.6
460	47.6
470	44.6

10.0 Test Set-Up Description

The following are the mobile antenna test configurations used for this product.
(for reference, see Illustration of antenna location and test distances in the appendix A)

- a) The 5/8 wave 3.5dBi gain antennas (PMAE4032A and PMAE4033A) and 5/8 wave 5.0dBi gain antenna (PMAE4034A) were assessed while mounted at the center of the roof of the test vehicle.
- b) The 5/8 wave 3.5dBi gain antennas (PMAE4032A and PMAE4033A) and 5/8 wave 5.0dBi gain antenna (PMAE4034A) were assessed while mounted at the center of the trunk of the test vehicle.

Assessments were made internal and external to the test vehicle at the specified distances and test locations indicated in sections 6.0, 11.0, and appendix A.

11.0 Test Results Summary

Appendix E presents detailed MPE measurement information for each test configuration; person external or internal to the vehicle, TX frequency, antenna (location, model and gain), distance from antenna to probe sensor, E field measurements, calibration factor, MPE average over body, initial power, power density calc, power density max calc, IEEE/FCC controlled and uncontrolled limits, and maximum output power.

The Average over Body test methodology is consistent with IEEE/ANSI C95.3-2002 guidelines.

MPE results are based on a 50% duty cycle which is in accordance with the User Manual instructions.

External to vehicle - 10 measurements are averaged over the body (*Body_Avg*).

Internal to vehicle - 3 measurements are averaged over the body (*Body_Avg*).

Narda Survey Meter measures in percent of the controlled limit. Therefore the averages over the body used in the calculations below reflect percentages.

MPE results are based on a Push-To-Talk (PTT) 50% duty cycle in CW mode.

Therefore;

$$\text{Average_over_Body} = \text{Body_Avg} * \text{Controlled_Limit}$$

$$\text{Pwr_Density_Calc} = \text{Average_over_Body} * \text{Duty_Cycle}$$

$$\text{Pwr_Density_Max_Calc} = \text{Pwr_Density_Calc} * \frac{\text{Max_Output_Power}}{\text{Initial_Output_Power}}$$

Note; For $\text{Initial Output Power} > \text{Max Output Power}$, $\text{Max Output Power} / \text{Initial Output Power} = 1$

The table below summarizes the MPE results of the E field test configurations for the PMUE2345A mobile radio. See appendices A and D respectively for test positions and detailed MPE measurement data.

Tables	Antenna Model	Antenna Location	Test Frequency (MHz)	E/H Field	Passenger / By-stander	Max Calc Pwr Density (mW/cm^2)	% of Uncontrolled Limit
Trunk Mount PMAE4032A							
1	PMAE4032A	Trunk	406	E	By-stander	0.12	44.3
*2	PMAE4032A	Trunk	406	E	Passenger	0.31	114.5
3	PMAE4032A	Trunk	416.5	E	By-stander	0.14	50.4
*4	PMAE4032A	Trunk	416.5	E	Passenger	0.37	133.3
5	PMAE4032A	Trunk	413	E	By-stander	0.11	40.0
*6	PMAE4032A	Trunk	413	E	Passenger	0.35	127.1
45 Degree From Trunk							
7	PMAE4032A	Trunk	416.5	E	By-stander	0.11	39.6
90 Degree From Trunk							
8	PMAE4032A	Trunk	416.5	E	By-stander	0.10	36.0
Trunk Mount PMAE4033A							
1	PMAE4033A	Trunk	450	E	By-stander	0.11	36.7
*2	PMAE4033A	Trunk	450	E	Passenger	0.54	180.0
3	PMAE4033A	Trunk	460	E	By-stander	0.14	45.7
*4	PMAE4033A	Trunk	460	E	Passenger	0.54	176.1
5	PMAE4033A	Trunk	470	E	By-stander	0.16	51.1
*6	PMAE4033A	Trunk	470	E	Passenger	0.43	137.2
45 Degree From Trunk							
7	PMAE4033A	Trunk	470	E	By-stander	0.12	38.3
90 Degree From Trunk							
8	PMAE4033A	Trunk	470	E	By-stander	0.12	38.3
Trunk Mount PMAE4034A							
1	PMAE4034A	Trunk	450	E	By-stander	0.10	33.3
*2	PMAE4034A	Trunk	450	E	Passenger	0.32	106.7
3	PMAE4034A	Trunk	460	E	By-stander	0.10	32.6
*4	PMAE4034A	Trunk	460	E	Passenger	0.34	110.9
5	PMAE4034A	Trunk	470	E	By-stander	0.14	44.7
*6	PMAE4034A	Trunk	470	E	Passenger	0.32	102.1
45 Degree From Trunk							
7	PMAE4034A	Trunk	470	E	By-stander	0.14	44.7
90 Degree From Trunk							
8	PMAE4034A	Trunk	470	E	By-stander	0.13	41.5

* Exceeds MPE General Population/Uncontrolled exposure limit

Table continued

Tables	Antenna Model	Antenna Location	Test Frequency (MHz)	E/H Field	Passenger / By-stander	Max Calc Pwr Density (mW/cm ²)	% of Uncontrolled Limit
Roof Mount PMAE4032A							
9	PMAE4032A	Roof	406	E	By-stander	0.06	22.2
10	PMAE4032A	Roof	406	E	Passenger	0.09	33.3
11	PMAE4032A	Roof	416.5	E	By-stander	0.10	36.0
12	PMAE4032A	Roof	416.5	E	Passenger	0.08	28.8
13	PMAE4032A	Roof	413	E	By-stander	0.08	29.1
14	PMAE4032A	Roof	413	E	Passenger	0.08	29.1
Roof Mount PMAE4033A							
9	PMAE4033A	Roof	450	E	By-stander	0.08	26.7
10	PMAE4033A	Roof	450	E	Passenger	0.06	20.0
11	PMAE4033A	Roof	460	E	By-stander	0.09	29.3
12	PMAE4033A	Roof	460	E	Passenger	0.06	19.6
13	PMAE4033A	Roof	470	E	By-stander	0.08	25.5
14	PMAE4033A	Roof	470	E	Passenger	0.05	16.0
Roof Mount PMAE4034A							
9	PMAE4034A	Roof	450	E	By-stander	0.08	26.7
10	PMAE4034A	Roof	450	E	Passenger	0.02	6.7
11	PMAE4034A	Roof	460	E	By-stander	0.09	29.3
12	PMAE4034A	Roof	460	E	Passenger	0.03	9.8
13	PMAE4034A	Roof	470	E	By-stander	0.08	25.5
14	PMAE4034A	Roof	470	E	Passenger	0.03	9.6

12.0 Conclusion

Depending on the test frequency, the PMUE2345A mobile assessments were performed with an output power range of 44.6W – 47.7W. The highest power density results for the PMUE2345A UHF mobile device scaled to the maximum allowable power output is 0.54mW/cm² internal to the vehicle and 0.16mW/cm² external to the vehicle.

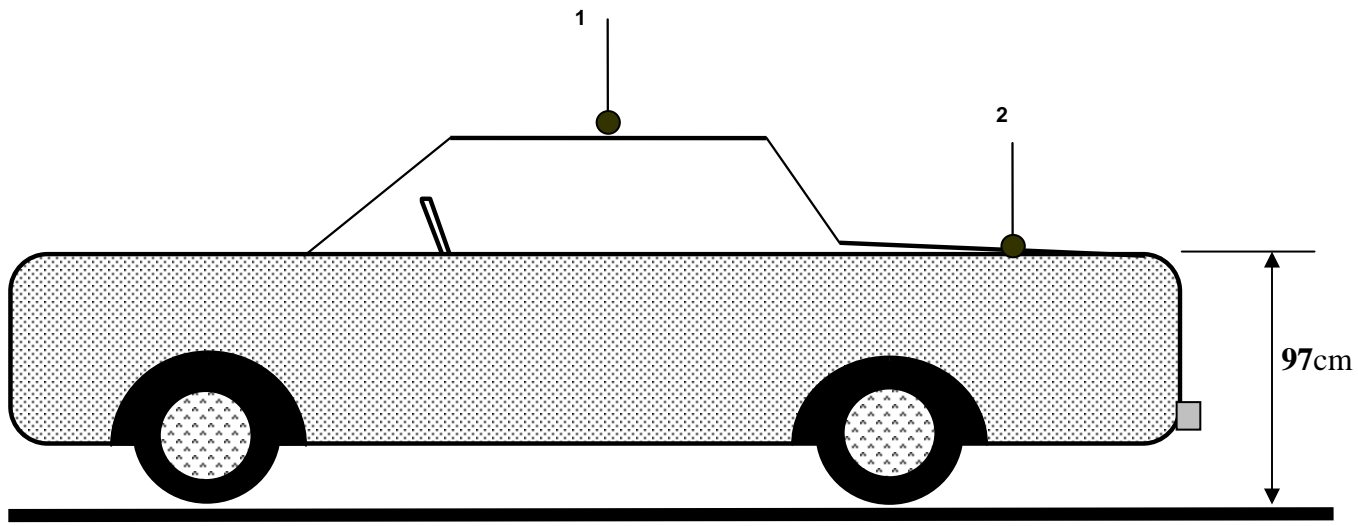
These MPE results demonstrate compliance to the FCC/IEEE Occupational/Controlled Exposure limit.

FCC rules require compliance for passengers and bystanders to the FCC General Population/Uncontrolled limits. Although MPE is a convenient method of demonstrating compliance, SAR is recognized as the "basic restriction". For those configurations exceeding the MPE limit noted in section 11.0 table, compliance to the FCC SAR General Population/Uncontrolled limit of 1.6mW/g is demonstrated in Part II Computational EME Compliance Assessment Via SAR computational analysis.

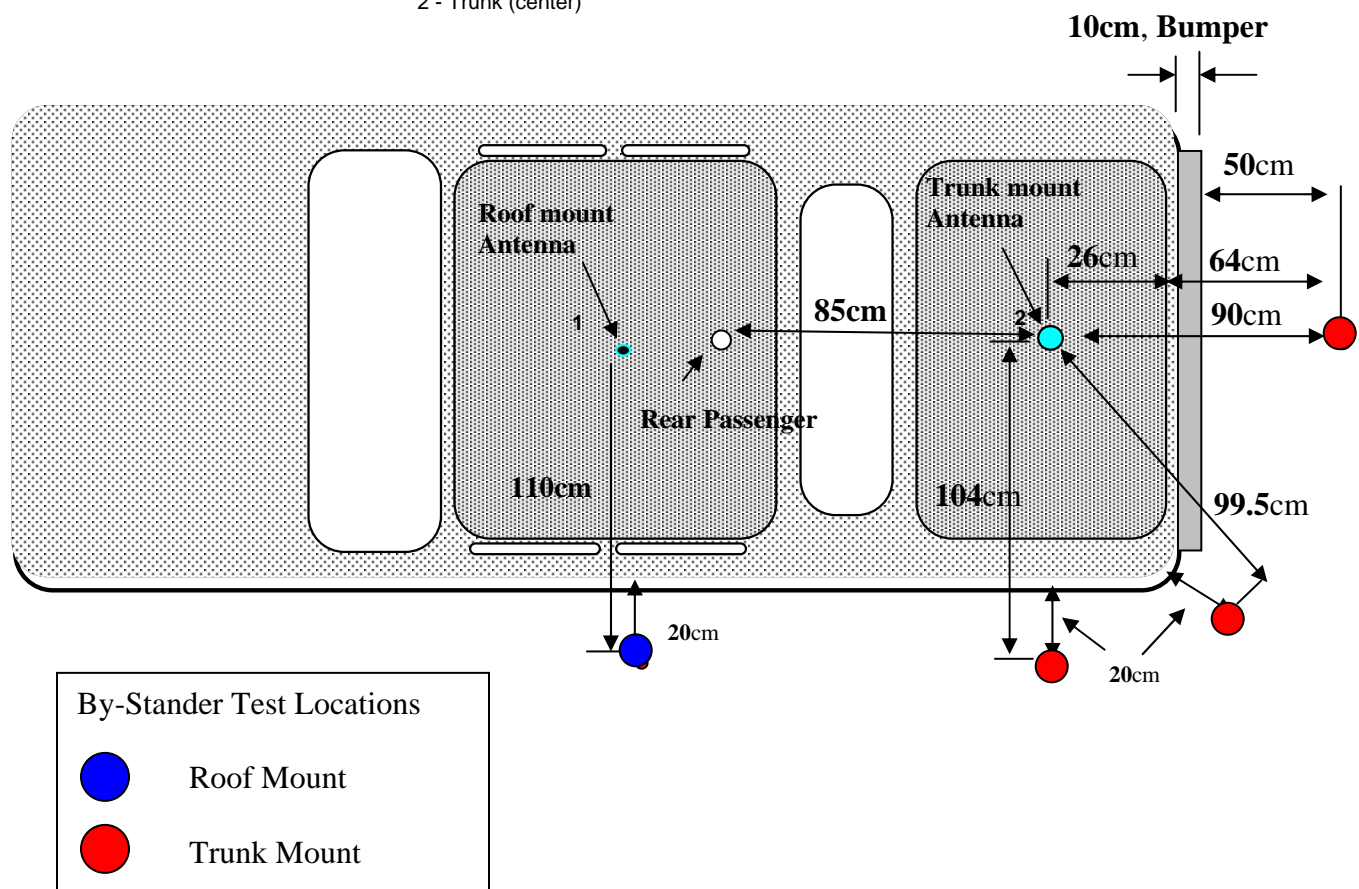
The computation results show that this device, when used with the specified antennas, exhibit a maximum combined peak 1-g average S.A.R. of 0.251mW/g.

APPENDIX A

Illustration of Antenna Locations and Test Distances



1 - Roof (center)
2 - Trunk (center)



APPENDIX B

Meter/Probe Calibration Certificates



Certificate of Calibration

L-3 Communications, Narda Microwave-East, hereby certifies that the referenced RF Radiation Hazard monitoring equipment has been calibrated in accordance with MIL-STD-45662A, ANSI Z540, ISO 10012 and ISO 9001: 2000.

The measured values were determined by comparison with our standards, which are traceable to the National Institute of Standards and Technology to the extent allowed by NIST's calibration facilities.

Customer: MOTOROLA
SCHAUMBURG, IL 60168-0429

Model #: 8718-10
Description: METER W/CABLE
Date Calibrated: 04/20/2006
R.O. #: 64777

Certificate #: 64777 1

Serial #: 01122
PO #: NP2398645

A handwritten signature in black ink, appearing to read 'Ken Peck'.

Ken Peck

Quality Assurance

A handwritten signature in black ink, appearing to read 'Vince Donavan'.

Vince Donavan

Manufacturing

This certificate shall not be reproduced, except in full, without written approval from L-3 Communications, Narda Microwave-East.



Certificate of Calibration

L-3 Communications, Narda Microwave-East, hereby certifies that the referenced RF Radiation Hazard monitoring equipment has been calibrated in accordance with MIL-STD-45662A, ANSI Z540, ISO 10012 and ISO 9001: 2000.

The measured values were determined by comparison with our standards, which are traceable to the National Institute of Standards and Technology to the extent allowed by NIST's calibration facilities.

Customer: MOTOROLA
SCHAUMBURG, IL 60168-0429

Model #: 8722B
Description: PROBE
Date Calibrated: 04/20/2006

Certificate #: 647772

Serial #: 12023
PO #: NP2398645
R.O. #: 64777

A handwritten signature in black ink, appearing to read 'Ken Peck'.

Ken Peck
Quality Assurance

A handwritten signature in black ink, appearing to read 'Vince Donovan'.

Vince Donovan
Manufacturing

This certificate shall not be reproduced, except in full, without written approval from L-3 Communications, Narda Microwave-East.



DATE 20-Apr-2006
REL HUMIDITY 46%

RELEASE # R64777
TEMP 21 DEG. C

NARDA MICROWAVE - EAST

MODEL # 8722B
SERIAL # 12023

FREQ MHZ	PRE-CAL DATA	FINAL CAL DATA	ELLIPSE RATIO, dB	FINAL CORR. FACTOR
.30	0.81	0.78	+/- 0.24	1.28
3.00	1.27	1.23	+/- 0.38	0.81
10.00	0.76	0.74	+/- 0.23	1.35
30.00	0.65	0.63	+/- 0.13	1.58
100.00	1.17	1.14	+/- 0.22	0.88
300.00	0.90	0.87	+/- 0.34	1.14
750.00	1.31	1.27	+/- 0.30	0.79
1000.00	1.63	1.58	+/- 0.35	0.63
1700.00	1.00	0.97	+/- 0.48	1.03
2450.00	1.35	1.37	+/- 0.45	0.73
4000.00	0.92	0.93	+/- 0.43	1.07
8200.00	1.05	1.07	+/- 0.46	0.94
10000.00	1.05	1.07	+/- 0.42	0.94
18000.00	1.17	1.19	+/- 0.75	0.84
26500.00	0.93	0.94	+/- 0.83	1.07
40000.00	0.72	0.73	+/- 0.67	1.37

LOW FREQUENCY MULTIPLIER = 0.972 HIGH FREQUENCY MULTIPLIER = 1.014

FREQ. DEV. (3-40000 MHZ) = 3.993 DB

FREQ. DEV. (0.3-40000 MHZ) = 3.99 DB

MAX. ELLIPSE RATIO (0.3-40000 MHZ) = +/- 0.83 DB

PRE-CAL DATA REFLECTS THE MEAN ELLIPSE RATIO OF PROBE AS RECEIVED BY NARDA CALIBRATION DEPARTMENT, OR IS THE INITIAL, UN-ADJUSTED RATIO.

(PRE-CAL x OLD CORR. FACTOR) - 1 = DEVIATION FROM PREVIOUS (OLD) CALIBRATION DATA. NOTE: NOT APPLICABLE FOR NEW PROBES.

FINAL CAL DATA IS THE RATIO OF THE DISPLAYED TO THE APPLIED FIELD STRENGTH.
FINAL CORR. FACTOR IS THE RECIPROCAL OF FINAL CAL DATA.

FINAL CORR. FACTOR MULTIPLIED BY THE DISPLAYED FIELD STRENGTH READING GIVES THE ACTUAL ("CORRECTED") FIELD STRENGTH.

ELLIPSE RATIO IS EXPRESSED IN dB DEVIATION FROM THE MEAN DATA

RMS Uncertainty = +/- 0.5db. ATP # = 502120 REVJ

TESTER L.V

Q.A. APPROVAL



APPENDIX C

Photos of Assessed Antennas



Antenna kit numbers; PMAE4032A

PMAE4033A

PMAE4034A

Note; Each antenna kit number includes GPS base PMAN4004A

APPENDIX D

Detailed MPE Measurement Data

Antenna PMAE4032A

Table 1

External Vehicle MPE Assessment @ 406 MHz									
Antenna Location	Antenna Model	Gain (dBi)	Meas. Distance (cm)	E/H Field	Calibration Factor	Average over Body (mW/cm^2)	Initial Power (W)	Pwr. Density Calc. (mW/cm^2)	Pwr. Density Max Calc. (mW/cm^2)
Trunk (cnt)	PMAE4032 A	5.65	90	E	1.06	0.234	47.7	0.117	0.12
Measurement Grid									
Test Position	Height (cm)	% of Control Limit	Test Position	Height (cm)	% of Control Limit		IEEE Controlled Limit	IEEE Uncontrolled Limit	
1	20	9.8%	6	120	25.3%		1.35	0.27	
2	40	10.1%	7	140	20.7%				
3	60	18.2%	8	160	17.7%				
4	80	20.0%	9	180	13.9%				
5	100	23.9%	10	200	13.5%				
							RF Po (*Max)		48.0

Table 2

Internal Vehicle MPE Assessment @ 406 MHz									
Antenna Location	Antenna	Gain (dBi)	Meas. Distance (cm)	E/H Field	Calibration Factor	Average over Head, Chest, Lower Trunk	Initial Power (W)	Pwr. Density Calc. (mW/cm^2)	Pwr. Density Max Calc. (mW/cm^2)
						Back/Front seats (mW/cm^2)			
Trunk (cnt)	PMAE4032 A	5.65	Highest Reading	E	1.06	0.612	0.238	47.7	0.306
									0.31
Measurement Grid									
Test Position	% of Control Limit Head		% of Control Limit Chest		% of Control Limit Lower Trunk		IEEE Controlled Limit:		1.35
Back Seat	66.6%		46.4%		22.6%		IEEE Uncontrolled Limit:		0.27
Front Seat	17.9%		15.5%		19.3%		RF Po (*Max):		48.0

Table 3

External Vehicle MPE Assessment @ 416.5 MHz									
Antenna Location	Antenna Model	Gain (dBi)	Meas. Distance (cm)	E/H Field	Calibration Factor	Average over Body (mW/cm^2)	Initial Power (W)	Pwr. Density Calc. (mW/cm^2)	Pwr. Density Max Calc. (mW/cm^2)
Trunk (cnt)	PMAE4032 A	5.65	90	E	1.05	0.266	47.2	0.133	0.14
Measurement Grid									
Test Position	Height (cm)	% of Control Limit	Test Position	Height (cm)	% of Control Limit		IEEE Controlled Limit	IEEE Uncontrolled Limit	
1	20	5.3%	6	120	25.9%		1.39	0.28	
2	40	7.7%	7	140	25.9%				
3	60	20.2%	8	160	23.2%				
4	80	24.1%	9	180	18.3%				
5	100	27.6%	10	200	13.7%				
					RF Po (*Max)				48.0

Antenna PMAE4032A

Table 4

Internal Vehicle MPE Assessment @ 416.5 MHz										
Antenna Location	Antenna	Gain (dBi)	Meas. Distance (cm)	E/H Field	Calibration Factor	Average over Head, Chest, Lower Trunk Back/Front seats (mW/cm^2)		Initial Power (W)	Pwr. Density Calc. (mW/cm^2)	Pwr. Density Max Calc. (mW/cm^2)
						Back	Front			
Trunk (cnt)	PMAE4032 A	5.65	Highest Reading	E	1.05	0.733	0.219	47.2	0.366	0.37
Measurement Grid										
Test Position		% of Control Limit Head		% of Control Limit Chest		% of Control Limit Lower Trunk		IEEE Controlled Limit:		
Back Seat		75.1%		40.5%		42.7%		IEEE Uncontrolled Limit:		
Front Seat		24.5%		8.5%		14.4%		RF Po (*Max):		

Table 5

External Vehicle MPE Assessment @ 413 MHz											
Antenna Location	Antenna Model	Gain (dBi)	Meas. Distance (cm)	E/H Field	Calibration Factor	Average over Body (mW/cm^2)	Initial Power (W)	Pwr. Density Calc. (mW/cm^2)	Pwr. Density Max Calc. (mW/cm^2)		
Trunk (cnt)	PMAE4032 A	5.65	90	E	1.05	0.212	47.1	0.106	0.11		
Measurement Grid											
Test Position	Height (cm)	% of Control Limit		Test Position	Height (cm)	% of Control Limit		IEEE Controlled Limit	IEEE Uncontrolled Limit		
1	20	6.3%		6	120	22.1%		1.38	0.28		
2	40	10.0%		7	140	17.4%		RF Po (*Max)	48.0		
3	60	16.8%		8	160	18.9%					
4	80	17.9%		9	180	14.5%					
5	100	19.5%		10	200	10.8%					

Table 6

Internal Vehicle MPE Assessment @ 413 MHz										
Antenna Location	Antenna	Gain (dBi)	Meas. Distance (cm)	E/H Field	Calibration Factor	Average over Head, Chest, Lower Trunk Back/Front seats (mW/cm^2)		Initial Power (W)	Pwr. Density Calc. (mW/cm^2)	Pwr. Density Max Calc. (mW/cm^2)
Antenna Location	Antenna	Gain (dBi)	Meas. Distance (cm)	E/H Field	Calibration Factor	Back	Front			
Trunk (cnt)	PMAE4032 A	5.65	Highest Reading	E	1.05	0.684	0.262	47.1	0.342	0.35
Measurement Grid										
Test Position	% of Control Limit Head		% of Control Limit Chest		% of Control Limit Lower Trunk		IEEE Controlled Limit:		1.38	
Back Seat	79.1%		42.7%		27.3%		IEEE Uncontrolled Limit:		0.28	
Front Seat	27.0%		10.2%		19.8%		RF Po (*Max):		48.0	

Antenna PMAE4032A

Use Worst case freq. from above (by-stander only)

Table 7 **45 degree

External Vehicle MPE Assessment @ 416.5 MHz									
Antenna Location	Antenna Model	Gain (dBi)	Meas. Distance (cm)	E/H Field	Calibration Factor	Average over Body (mW/cm^2)	Initial Power (W)	Pwr. Density Calc. (mW/cm^2)	Pwr. Density Max Calc. (mW/cm^2)
Trunk (cnt)	PMAE4032 A	5.65	90 (actual 99.5)	E	1.05	0.222	47.2	0.111	0.11
Measurement Grid									
Test Position	Height (cm)	% of Control Limit	Test Position	Height (cm)	% of Control Limit	IEEE Controlled Limit	IEEE Uncontrolled Limit	RF Po (*Max)	
1	20	9.1%	6	120	20.0%	1.39	0.28	48.0	
2	40	11.7%	7	140	19.8%				
3	60	13.5%	8	160	19.7%				
4	80	15.1%	9	180	17.7%				
5	100	18.4%	10	200	14.9%				

Use Worst case freq. from above (by-stander only)

Table 8 **90 degree

External Vehicle MPE Assessment @ 416.5 MHz									
Antenna Location	Antenna Model	Gain (dBi)	Meas. Distance (cm)	E/H Field	Calibration Factor	Average over Body (mW/cm^2)	Initial Power (W)	Pwr. Density Calc. (mW/cm^2)	Pwr. Density Max Calc. (mW/cm^2)
Trunk (cnt)	PMAE4032 A	5.65	90 (actual 104)	E	1.05	0.201	47.2	0.100	0.10
Measurement Grid									
Test Position	Height (cm)	% of Control Limit	Test Position	Height (cm)	% of Control Limit	IEEE Controlled Limit	IEEE Uncontrolled Limit	RF Po (*Max)	
1	20	8.4%	6	120	18.8%	1.39	0.28	48.0	
2	40	8.0%	7	140	20.1%				
3	60	10.5%	8	160	19.9%				
4	80	12.7%	9	180	17.8%				
5	100	14.7%	10	200	13.6%				

Antenna PMAE4032A

Table 9

External Vehicle MPE Assessment @ 406 MHz								
Antenna Location	Antenna Model	Gain (dBi)	Meas. Distance (cm)	E/H Field	Calibration Factor	Average over Body (mW/cm^2)	Initial Power (W)	Pwr. Density Calc. (mW/cm^2)
Roof (cnt)	PMAE4032 A	5.65	90 (actual 110)	E	1.06	0.124	47.7	0.062
Measurement Grid								
Test Position	Height (cm)	% of Control Limit	Test Position	Height (cm)	% of Control Limit	IEEE Controlled Limit	IEEE Uncontrolled Limit	
1	20	1.8%	6	120	10.6%	1.35	0.27	
2	40	2.1%	7	140	12.5%			
3	60	4.4%	8	160	14.0%			
4	80	6.2%	9	180	15.4%			RF Po (*Max)
5	100	8.1%	10	200	16.3%		48.0	

Table 10

Internal Vehicle MPE Assessment @ 406 MHz								
Antenna Location	Antenna	Gain (dBi)	Meas. Distance (cm)	E/H Field	Calibration Factor	Average over Head, Chest, Lower Trunk Back/Front seats (mW/cm^2)	Initial Power (W)	Pwr. Density Calc. (mW/cm^2)
Roof (cnt)	PMAE4032 A	5.65	Highest Reading	E	1.06	0.173	0.147	47.7
Measurement Grid								
Test Position	% of Control Limit Head		% of Control Limit Chest		% of Control Limit Lower Trunk		IEEE Controlled Limit:	1.35
Back Seat	17.4%		8.8%		12.2%		IEEE Uncontrolled Limit:	0.27
Front Seat	19.0%		4.4%		9.2%		RF Po (*Max):	48.0

Table 11

External Vehicle MPE Assessment @ 416.5 MHz								
Antenna Location	Antenna Model	Gain (dBi)	Meas. Distance (cm)	E/H Field	Calibration Factor	Average over Body (mW/cm^2)	Initial Power (W)	Pwr. Density Calc. (mW/cm^2)
Roof (cnt)	PMAE4032 A	5.65	90 (actual 110)	E	1.05	0.190	47.2	0.095
Measurement Grid								
Test Position	Height (cm)	% of Control Limit	Test Position	Height (cm)	% of Control Limit	IEEE Controlled Limit	IEEE Uncontrolled Limit	
1	20	3.4%	6	120	15.9%	1.39	0.28	
2	40	2.5%	7	140	19.2%			
3	60	5.8%	8	160	24.3%			
4	80	6.2%	9	180	24.1%			RF Po (*Max)
5	100	10.6%	10	200	25.0%		48.0	

Antenna PMAE4032A

Table 12

Internal Vehicle MPE Assessment @ 416.5 MHz										
Antenna Location	Antenna	Gain (dBi)	Meas. Distance (cm)	E/H Field	Calibration Factor	Average over Head, Chest, Lower Trunk Back/Front seats (mW/cm^2)		Initial Power (W)	Pwr. Density Calc. (mW/cm^2)	Pwr. Density Max Calc. (mW/cm^2)
						Back	Front			
Roof (cnt)	PMAE4032 A	5.65	Highest Reading	E	1.05	0.127	0.156	47.2	0.078	0.08

Measurement Grid									
Test Position		% of Control Limit Head		% of Control Limit Chest		% of Control Limit Lower Trunk		IEEE Controlled Limit:	
Back Seat		12.1%		8.8%		6.5%		IEEE Uncontrolled Limit:	
Front Seat		14.5%		6.9%		12.4%		RF Po (*Max):	

Table 13

External Vehicle MPE Assessment @ 413 MHz									
Antenna Location	Antenna Model	Gain (dBi)	Meas. Distance (cm)	E/H Field	Calibration Factor	Average over Body (mW/cm^2)	Initial Power (W)	Pwr. Density Calc. (mW/cm^2)	Pwr. Density Max Calc. (mW/cm^2)
Roof (cnt)	PMAE4032 A	5.65	90 (actual 110)	E	1.05	0.150	47.1	0.075	0.08

Measurement Grid											
Test Position		% of Control Limit Head		Test Position		% of Control Limit		IEEE Controlled Limit:			
1	20	2.5%		6	120	11.1%		1.38	0.28		
2	40	2.6%		7	140	16.4%		RF Po (*Max)	48.0		
3	60	5.0%		8	160	17.7%					
4	80	6.4%		9	180	20.1%					
5	100	7.0%		10	200	20.5%					

Table 14

Internal Vehicle MPE Assessment @ 413 MHz										
Antenna Location	Antenna	Gain (dBi)	Meas. Distance (cm)	E/H Field	Calibration Factor	Average over Head, Chest, Lower Trunk Back/Front seats (mW/cm^2)		Initial Power (W)	Pwr. Density Calc. (mW/cm^2)	Pwr. Density Max Calc. (mW/cm^2)
						Back	Front			
Roof (cnt)	PMAE4032 A	5.65	Highest Reading	E	1.05	0.119	0.150	47.1	0.075	0.08

Measurement Grid									
Test Position		% of Control Limit Head		% of Control Limit Chest		% of Control Limit Lower Trunk		IEEE Controlled Limit:	
Back Seat		11.5%		7.3%		7.2%		IEEE Uncontrolled Limit:	
Front Seat		14.0%		6.1%		12.5%		RF Po (*Max):	

Antenna PMAE4033A

Table 1

External Vehicle MPE Assessment @ 450 MHz							
Antenna Location	Antenna Model	Gain (dBi)	Meas. Distance (cm)	E/H Field	Calibration Factor		
Trunk (cnt)	PMAE4033 A	5.65	90	E	1.02		
Measurement Grid							
Test Position	Height (cm)	% of Control Limit	Test Position	Height (cm)	% of Control Limit	IEEE Controlled Limit	IEEE Uncontrolled Limit
1	20	5.8%	6	120	20.1%	1.50	0.30
2	40	10.7%	7	140	22.4%	RF Po (*Max)	48.0
3	60	14.9%	8	160	17.5%		
4	80	14.1%	9	180	13.9%		
5	100	13.6%	10	200	9.4%		

Table 2

Internal Vehicle MPE Assessment @ 450 MHz										
Antenna Location	Antenna	Gain (dBi)	Meas. Distance (cm)	E/H Field	Calibration Factor	Average over Head, Chest, Lower Trunk Back/Front seats (mW/cm^2)		Initial Power (W)	Pwr. Density Calc. (mW/cm^2)	Pwr. Density Max Calc. (mW/cm^2)
						Back	Front			
Trunk (cnt)	PMAE4033 A	5.65	Highest Reading	E	1.02	1.072	0.732	47.6	0.536	0.54
Measurement Grid										
Test Position		% of Control Limit Head		% of Control Limit Chest		% of Control Limit Lower Trunk		IEEE Controlled Limit:		1.50
Back Seat		81.1%		81.9%		51.4%		IEEE Uncontrolled Limit:		0.30
Front Seat		65.1%		31.6%		49.7%		RF Po (*Max):		48.0

Table 3

External Vehicle MPE Assessment @ 460 MHz							
Antenna Location	Antenna Model	Gain (dBi)	Meas. Distance (cm)	E/H Field	Calibration Factor		
Trunk (cnt)	PMAE4033 A	5.65	90	E	1.02		
Measurement Grid							
Test Position	Height (cm)	% of Control Limit	Test Position	Height (cm)	% of Control Limit	IEEE Controlled Limit	IEEE Uncontrolled Limit
1	20	5.9%	6	120	27.2%	1.53	0.31
2	40	10.3%	7	140	28.7%	RF Po (*Max)	48.0
3	60	16.3%	8	160	26.5%		
4	80	17.3%	9	180	18.4%		
5	100	19.0%	10	200	9.4%		

Antenna PMAE4033A

Table 4

Internal Vehicle MPE Assessment @ 460 MHz										
Antenna Location	Antenna	Gain (dBi)	Meas. Distance (cm)	E/H Field	Calibration Factor	Average over Head, Chest, Lower Trunk Back/Front seats (mW/cm^2)		Initial Power (W)	Pwr. Density Calc. (mW/cm^2)	Pwr. Density Max Calc. (mW/cm^2)
						Back	Front			
Trunk (cnt)	PMAE4033 A	5.65	Highest Reading	E	1.02	1.063	0.792	47.6	0.531	0.54
Measurement Grid										
Test Position		% of Control Limit Head		% of Control Limit Chest		% of Control Limit Lower Trunk		IEEE Controlled Limit:		
Back Seat		89.6%		67.9%		50.4%		IEEE Uncontrolled Limit:		
Front Seat		61.6%		22.7%		70.7%		RF Po (*Max):		

Table 5

External Vehicle MPE Assessment @ 470 MHz									
Antenna Location	Antenna Model	Gain (dBi)	Meas. Distance (cm)	E/H Field	Calibration Factor	Average over Body (mW/cm^2)	Initial Power (W)	Pwr. Density Calc. (mW/cm^2)	Pwr. Density Max Calc. (mW/cm^2)
Trunk (cnt)	PMAE4033 A	5.65	90	E	1.01	0.300	44.6	0.150	0.16
Measurement Grid									
Test Position	Height (cm)	% of Control Limit	Test Position	Height (cm)	% of Control Limit	IEEE Controlled Limit	IEEE Uncontrolled Limit		
1	20	6.3%	6	120	27.6%	1.57	0.31		
2	40	9.2%	7	140	32.2%				
3	60	13.9%	8	160	30.7%				
4	80	14.7%	9	180	22.2%			RF Po (*Max)	
5	100	22.8%	10	200	12.0%			48.0	

Table 6

Internal Vehicle MPE Assessment @ 470 MHz										
Antenna Location	Antenna	Gain (dBi)	Meas. Distance (cm)	E/H Field	Calibration Factor	Average over Head, Chest, Lower Trunk Back/Front seats (mW/cm^2)	Initial Power (W)	Pwr. Density Calc. (mW/cm^2)	Pwr. Density Max Calc. (mW/cm^2)	
Trunk (cnt)	PMAE4033 A	5.65	Highest Reading	E	1.01	0.792	0.574	44.6	0.396	0.43
Measurement Grid										
Test Position	% of Control Limit Head		% of Control Limit Chest		% of Control Limit Lower Trunk		IEEE Controlled Limit:		1.57	
Back Seat	61.6%		56.8%		33.3%		IEEE Uncontrolled Limit:		0.31	
Front Seat	42.1%		19.4%		48.5%		RF Po (*Max):		48.0	

Antenna PMAE4033A

Use Worst case freq. from above (by-stander only)

Table 7 **45 degree

External Vehicle MPE Assessment @ 470 MHz											
Antenna Location	Antenna Model	Gain (dBi)	Meas. Distance (cm)	E/H Field	Calibration Factor	Average over Body (mW/cm^2)	Initial Power (W)	Pwr. Density Calc. (mW/cm^2)	Pwr. Density Max Calc. (mW/cm^2)		
Trunk (cnt)	PMAE4033 A	5.65	90 (actual 99.5)	E	1.01	0.231	44.6	0.116	0.12		
Measurement Grid											
Test Position	Height (cm)	% of Control Limit		Test Position	Height (cm)	% of Control Limit		IEEE Controlled Limit	IEEE Uncontrolled Limit		
1	20	5.5%		6	120	18.0%		1.57	0.31		
2	40	7.3%		7	140	21.5%		RF Po (*Max)	48.0		
3	60	10.0%		8	160	23.0%					
4	80	15.1%		9	180	18.4%					
5	100	15.8%		10	200	12.9%					

Use Worst case freq. from above (by-stander only)

Table 8 **90 degree

External Vehicle MPE Assessment @ 470 MHz											
Antenna Location	Antenna Model	Gain (dBi)	Meas. Distance (cm)	E/H Field	Calibration Factor	Average over Body (mW/cm^2)	Initial Power (W)	Pwr. Density Calc. (mW/cm^2)	Pwr. Density Max Calc. (mW/cm^2)		
Trunk (cnt)	PMAE4033 A	5.65	90 (actual 104)	E	1.01	0.219	44.6	0.110	0.12		
Measurement Grid											
Test Position	Height (cm)	% of Control Limit		Test Position	Height (cm)	% of Control Limit		IEEE Controlled Limit	IEEE Uncontrolled Limit		
1	20	5.2%		6	120	16.2%		1.57	0.31		
2	40	7.0%		7	140	20.5%		RF Po (*Max)	48.0		
3	60	10.6%		8	160	21.7%					
4	80	14.8%		9	180	17.8%					
5	100	15.9%		10	200	10.2%					

Antenna PMAE4033A

Table 9

External Vehicle MPE Assessment @ 450 MHz											
Antenna Location	Antenna Model	Gain (dBi)	Meas. Distance (cm)	E/H Field	Calibration Factor	Average over Body (mW/cm^2)	Initial Power (W)	Pwr. Density Calc. (mW/cm^2)	Pwr. Density Max Calc. (mW/cm^2)		
Roof (cnt)	PMAE4033 A	5.65	90 (actual 110)	E	1.02	0.152	47.6	0.076	0.08		
Measurement Grid											
Test Position	Height (cm)	% of Control Limit		Test Position	Height (cm)	% of Control Limit		IEEE Controlled Limit	IEEE Uncontrolled Limit		
1	20	2.1%		6	120	9.6%		1.50	0.30		
2	40	3.1%		7	140	12.5%		RF Po (*Max)	48.0		
3	60	6.4%		8	160	16.3%					
4	80	6.1%		9	180	18.3%					
5	100	7.0%		10	200	20.0%					

Table 10

Internal Vehicle MPE Assessment @ 450 MHz											
Antenna Location	Antenna	Gain (dBi)	Meas. Distance (cm)	E/H Field	Calibration Factor	Average over Head, Chest, Lower Trunk Back/Front seats (mW/cm^2)		Initial Power (W)	Pwr. Density Calc. (mW/cm^2)	Pwr. Density Max Calc. (mW/cm^2)	
						Back	Front				
Roof (cnt)	PMAE4033 A	5.65	Highest Reading	E	1.02	0.117	0.078	47.6	0.058	0.06	
Measurement Grid											
Test Position	% of Control Limit Head		% of Control Limit Chest		% of Control Limit Lower Trunk		IEEE Controlled Limit:			1.50	
Back Seat	6.1%		6.5%		10.7%		IEEE Uncontrolled Limit:			0.30	
Front Seat	4.8%		4.0%		6.8%		RF Po (*Max):			48.0	

Table 11

External Vehicle MPE Assessment @ 460 MHz											
Antenna Location	Antenna Model	Gain (dBi)	Meas. Distance (cm)	E/H Field	Calibration Factor	Average over Body (mW/cm^2)	Initial Power (W)	Pwr. Density Calc. (mW/cm^2)	Pwr. Density Max Calc. (mW/cm^2)		
Roof (cnt)	PMAE4033 A	5.65	90 (actual 110)	E	1.02	0.176	47.6	0.088	0.09		
Measurement Grid											
Test Position	Height (cm)	% of Control Limit		Test Position	Height (cm)	% of Control Limit		IEEE Controlled Limit	IEEE Uncontrolled Limit		
1	20	2.0%		6	120	10.9%		1.53	0.31		
2	40	2.2%		7	140	12.5%		RF Po (*Max)	48.0		
3	60	5.3%		8	160	18.3%					
4	80	5.8%		9	180	24.4%					
5	100	9.7%		10	200	23.7%					

Antenna PMAE4033A

Table 12

Internal Vehicle MPE Assessment @ 460 MHz										
Antenna Location	Antenna	Gain (dBi)	Meas. Distance (cm)	E/H Field	Calibration Factor	Average over Head, Chest, Lower Trunk Back/Front seats (mW/cm^2)		Initial Power (W)	Pwr. Density Calc. (mW/cm^2)	Pwr. Density Max Calc. (mW/cm^2)
						Back	Front			
Roof (cnt)	PMAE4033 A	5.65	Highest Reading	E	1.02	0.124	0.117	47.6	0.062	0.06
Measurement Grid										
Test Position		% of Control Limit Head		% of Control Limit Chest		% of Control Limit Lower Trunk		IEEE Controlled Limit:		
Back Seat		5.3%		9.9%		9.0%		IEEE Uncontrolled Limit:		
Front Seat		6.2%		4.6%		12.0%		RF Po (*Max):		

Table 13

External Vehicle MPE Assessment @ 470 MHz											
Antenna Location	Antenna Model	Gain (dBi)	Meas. Distance (cm)	E/H Field	Calibration Factor	Average over Body (mW/cm^2)	Initial Power (W)	Pwr. Density Calc. (mW/cm^2)	Pwr. Density Max Calc. (mW/cm^2)		
Roof (cnt)	PMAE4033 A	5.65	90 (actual 110)	E	1.01	0.143	44.6	0.071	0.08		
Measurement Grid											
Test Position	Height (cm)	% of Control Limit		Test Position	Height (cm)	% of Control Limit		IEEE Controlled Limit	IEEE Uncontrolled Limit		
1	20	1.5%		6	120	9.9%		1.57	0.31		
2	40	2.3%		7	140	12.3%		RF Po (*Max)	48.0		
3	60	3.3%		8	160	15.0%					
4	80	5.2%		9	180	18.4%					
5	100	5.7%		10	200	17.5%					

Table 14

Internal Vehicle MPE Assessment @ 470 MHz										
Antenna Location	Antenna	Gain (dBi)	Meas. Distance (cm)	E/H Field	Calibration Factor	Average over Head, Chest, Lower Trunk Back/Front seats (mW/cm^2)		Initial Power (W)	Pwr. Density Calc. (mW/cm^2)	Pwr. Density Max Calc. (mW/cm^2)
						Back	Front			
Roof (cnt)	PMAE4033 A	5.65	Highest Reading	E	1.01	0.098	0.088	44.6	0.049	0.05
Measurement Grid										
Test Position	% of Control Limit Head		% of Control Limit Chest		% of Control Limit Lower Trunk		IEEE Controlled Limit:		1.57	
Back Seat	5.8%		6.7%		6.2%		IEEE Uncontrolled Limit:		0.31	
Front Seat	3.4%		4.5%		8.9%		RF Po (*Max):		48.0	

Antenna PMAE4034A

Table 1

External Vehicle MPE Assessment @ 450 MHz								
Antenna Location	Antenna Model	Gain (dBi)	Meas. Distance (cm)	E/H Field	Calibration Factor	Average over Body (mW/cm^2)	Initial Power (W)	Pwr. Density Calc. (mW/cm^2)
Trunk (cnt)	PMAE4034 A	7.15	90	E	1.02	0.194	47.6	0.097
Measurement Grid								
Test Position	Height (cm)	% of Control Limit	Test Position	Height (cm)	% of Control Limit	IEEE Controlled Limit	IEEE Uncontrolled Limit	
1	20	1.0%	6	120	24.9%	1.50	0.30	
2	40	2.7%	7	140	33.8%			
3	60	3.7%	8	160	26.0%			
4	80	7.2%	9	180	10.6%			RF Po (*Max)
5	100	17.4%	10	200	2.2%		48.0	

Table 2

Internal Vehicle MPE Assessment @ 450 MHz								
Antenna Location	Antenna	Gain (dBi)	Meas. Distance (cm)	E/H Field	Calibration Factor	Average over Head, Chest, Lower Trunk	Initial Power (W)	Pwr. Density Calc. (mW/cm^2)
						Back/Front seats (mW/cm^2)		
Trunk (cnt)	PMAE4034 A	7.15	Highest Reading	E	1.02	0.628	0.371	47.6
Measurement Grid								
Test Position	% of Control Limit Head		% of Control Limit Chest		% of Control Limit Lower Trunk		IEEE Controlled Limit:	1.50
Back Seat	43.4%		51.3%		30.8%		IEEE Uncontrolled Limit:	0.30
Front Seat	32.1%		13.6%		28.5%		RF Po (*Max):	48.0

Table 3

External Vehicle MPE Assessment @ 460 MHz								
Antenna Location	Antenna Model	Gain (dBi)	Meas. Distance (cm)	E/H Field	Calibration Factor	Average over Body (mW/cm^2)	Initial Power (W)	Pwr. Density Calc. (mW/cm^2)
Trunk (cnt)	PMAE4034 A	7.15	90	E	1.02	0.202	47.6	0.101
Measurement Grid								
Test Position	Height (cm)	% of Control Limit	Test Position	Height (cm)	% of Control Limit	IEEE Controlled Limit	IEEE Uncontrolled Limit	
1	20	2.5%	6	120	21.4%	1.53	0.31	
2	40	3.0%	7	140	32.5%			
3	60	5.4%	8	160	30.4%			
4	80	6.3%	9	180	12.4%			RF Po (*Max)
5	100	15.5%	10	200	2.4%		48.0	

Antenna PMAE4034A

Table 4

Internal Vehicle MPE Assessment @ 460 MHz										
Antenna Location	Antenna	Gain (dBi)	Meas. Distance (cm)	E/H Field	Calibration Factor	Average over Head, Chest, Lower Trunk Back/Front seats (mW/cm^2)		Initial Power (W)	Pwr. Density Calc. (mW/cm^2)	Pwr. Density Max Calc. (mW/cm^2)
						Back	Front			
Trunk (cnt)	PMAE4034 A	7.15	Highest Reading	E	1.02	0.679	0.492	47.6	0.340	0.34
Measurement Grid										
Test Position		% of Control Limit Head		% of Control Limit Chest		% of Control Limit Lower Trunk		IEEE Controlled Limit:		
Back Seat		59.2%		47.1%		26.6%		IEEE Uncontrolled Limit:		
Front Seat		38.8%		15.5%		42.0%		RF Po (*Max):		

Table 5

External Vehicle MPE Assessment @ 470 MHz											
Antenna Location	Antenna Model	Gain (dBi)	Meas. Distance (cm)	E/H Field	Calibration Factor	Average over Body (mW/cm^2)	Initial Power (W)	Pwr. Density Calc. (mW/cm^2)	Pwr. Density Max Calc. (mW/cm^2)		
Trunk (cnt)	PMAE4034 A	7.15	90	E	1.01	0.257	44.6	0.129	0.14		
Measurement Grid											
Test Position	Height (cm)	% of Control Limit		Test Position	Height (cm)	% of Control Limit		IEEE Controlled Limit	IEEE Uncontrolled Limit		
1	20	3.4%		6	120	28.6%		1.57	0.31		
2	40	4.5%		7	140	39.5%		RF Po (*Max)	48.0		
3	60	6.1%		8	160	33.5%					
4	80	9.9%		9	180	16.8%					
5	100	19.0%		10	200	3.0%					

Table 6

Internal Vehicle MPE Assessment @ 470 MHz										
Antenna Location	Antenna	Gain (dBi)	Meas. Distance (cm)	E/H Field	Calibration Factor	Average over Head, Chest, Lower Trunk Back/Front seats (mW/cm^2)	Initial Power (W)	Pwr. Density Calc. (mW/cm^2)	Pwr. Density Max Calc. (mW/cm^2)	
Antenna Location	Antenna	Gain (dBi)	Meas. Distance (cm)	E/H Field	Calibration Factor					
Trunk (cnt)	PMAE4034 A	7.15	Highest Reading	E	1.01	0.602	0.474	44.6	0.301	0.32
Measurement Grid										
Test Position	% of Control Limit Head		% of Control Limit Chest		% of Control Limit Lower Trunk		IEEE Controlled Limit:		1.57	
Back Seat	48.3%		41.7%		25.3%		IEEE Uncontrolled Limit:		0.31	
Front Seat	29.2%		13.4%		48.2%		RF Po (*Max):		48.0	

Antenna PMAE4034A

Use Worst case freq. from above (by-stander only)

Table 7 **45 degree

External Vehicle MPE Assessment @ 470 MHz											
Antenna Location	Antenna Model	Gain (dBi)	Meas. Distance (cm)	E/H Field	Calibration Factor	Average over Body (mW/cm^2)	Initial Power (W)	Pwr. Density Calc. (mW/cm^2)	Pwr. Density Max Calc. (mW/cm^2)		
Trunk (cnt)	PMAE4034 A	7.15	90 (actual 99.5)	E	1.01	0.260	44.6	0.130	0.14		
Measurement Grid											
Test Position	Height (cm)	% of Control Limit		Test Position	Height (cm)	% of Control Limit		IEEE Controlled Limit	IEEE Uncontrolled Limit		
1	20	2.4%		6	120	25.3%		1.57	0.31		
2	40	3.0%		7	140	33.3%		RF Po (*Max)	48.0		
3	60	7.1%		8	160	31.8%					
4	80	13.5%		9	180	21.1%					
5	100	19.0%		10	200	9.3%					

Use Worst case freq. from above (by-stander only)

Table 8 **90 degree

External Vehicle MPE Assessment @ 470 MHz											
Antenna Location	Antenna Model	Gain (dBi)	Meas. Distance (cm)	E/H Field	Calibration Factor	Average over Body (mW/cm^2)	Initial Power (W)	Pwr. Density Calc. (mW/cm^2)	Pwr. Density Max Calc. (mW/cm^2)		
Trunk (cnt)	PMAE4034 A	7.15	90 (actual 104)	E	1.01	0.236	44.6	0.118	0.13		
Measurement Grid											
Test Position	Height (cm)	% of Control Limit		Test Position	Height (cm)	% of Control Limit		IEEE Controlled Limit	IEEE Uncontrolled Limit		
1	20	3.7%		6	120	22.5%		1.57	0.31		
2	40	4.7%		7	140	26.6%		RF Po (*Max)	48.0		
3	60	8.5%		8	160	27.4%					
4	80	11.2%		9	180	19.7%					
5	100	16.0%		10	200	10.3%					

Antenna PMAE4034A

Table 9

External Vehicle MPE Assessment @ 450 MHz											
Antenna Location	Antenna Model	Gain (dBi)	Meas. Distance (cm)	E/H Field	Calibration Factor	Average over Body (mW/cm^2)	Initial Power (W)	Pwr. Density Calc. (mW/cm^2)	Pwr. Density Max Calc. (mW/cm^2)		
Roof (cnt)	PMAE4034 A	7.15	90 (actual 110)	E	1.02	0.168	47.6	0.084	0.08		
Measurement Grid											
Test Position	Height (cm)	% of Control Limit		Test Position	Height (cm)	% of Control Limit		IEEE Controlled Limit	IEEE Uncontrolled Limit		
1	20	1.4%		6	120	11.6%		1.50	0.30		
2	40	1.4%		7	140	13.9%		RF Po (*Max)	48.0		
3	60	3.3%		8	160	20.2%					
4	80	3.8%		9	180	26.6%					
5	100	5.3%		10	200	24.2%					

Table 10

Internal Vehicle MPE Assessment @ 450 MHz										
Antenna Location	Antenna	Gain (dBi)	Meas. Distance (cm)	E/H Field	Calibration Factor	Average over Head, Chest, Lower Trunk Back/Front seats (mW/cm^2)		Initial Power (W)	Pwr. Density Calc. (mW/cm^2)	Pwr. Density Max Calc. (mW/cm^2)
						Back	Front			
Roof (cnt)	PMAE4034 A	7.15	Highest Reading	E	1.02	0.042	0.036	47.6	0.021	0.02
Measurement Grid										
Test Position		% of Control Limit Head		% of Control Limit Chest		% of Control Limit Lower Trunk		IEEE Controlled Limit:		
Back Seat		2.3%		2.4%		3.6%		IEEE Uncontrolled Limit:		
Front Seat		2.1%		2.0%		3.0%		RF Po (*Max):		

Table 11

External Vehicle MPE Assessment @ 460 MHz											
Antenna Location	Antenna Model	Gain (dBi)	Meas. Distance (cm)	E/H Field	Calibration Factor	Average over Body (mW/cm^2)	Initial Power (W)	Pwr. Density Calc. (mW/cm^2)	Pwr. Density Max Calc. (mW/cm^2)		
Roof (cnt)	PMAE4034 A	7.15	90 (actual 110)	E	1.02	0.169	47.6	0.085	0.09		
Measurement Grid											
Test Position	Height (cm)	% of Control Limit		Test Position	Height (cm)	% of Control Limit		IEEE Controlled Limit	IEEE Uncontrolled Limit		
1	20	1.2%		6	120	10.4%		1.53	0.31		
2	40	1.4%		7	140	16.0%		RF Po (*Max)	48.0		
3	60	2.4%		8	160	21.8%					
4	80	2.5%		9	180	27.9%					
5	100	5.3%		10	200	21.6%					

Antenna PMAE4034A

Table 12

Internal Vehicle MPE Assessment @ 460 MHz										
Antenna Location	Antenna	Gain (dBi)	Meas. Distance (cm)	E/H Field	Calibration Factor	Average over Head, Chest, Lower Trunk Back/Front seats (mW/cm^2)		Initial Power (W)	Pwr. Density Calc. (mW/cm^2)	Pwr. Density Max Calc. (mW/cm^2)
						Back	Front			
Roof (cnt)	PMAE4034 A	7.15	Highest Reading	E	1.02	0.044	0.056	47.6	0.028	0.03
Measurement Grid										
Test Position		% of Control Limit Head		% of Control Limit Chest		% of Control Limit Lower Trunk		IEEE Controlled Limit:		
Back Seat		2.7%		2.9%		3.1%		IEEE Uncontrolled Limit:		
Front Seat		3.3%		2.5%		5.2%		RF Po (*Max):		

Table 13

External Vehicle MPE Assessment @ 470 MHz											
Antenna Location	Antenna Model	Gain (dBi)	Meas. Distance (cm)	E/H Field	Calibration Factor	Average over Body (mW/cm^2)	Initial Power (W)	Pwr. Density Calc. (mW/cm^2)	Pwr. Density Max Calc. (mW/cm^2)		
Roof (cnt)	PMAE4034 A	7.15	90 (actual 110)	E	1.01	0.142	44.6	0.071	0.08		
Measurement Grid											
Test Position	Height (cm)	% of Control Limit		Test Position	Height (cm)	% of Control Limit		IEEE Controlled Limit	IEEE Uncontrolled Limit		
1	20	1.4%		6	120	7.5%		1.57	0.31		
2	40	1.8%		7	140	10.9%		RF Po (*Max)	48.0		
3	60	2.2%		8	160	18.1%					
4	80	3.8%		9	180	19.5%					
5	100	4.7%		10	200	20.7%					

Table 14

Internal Vehicle MPE Assessment @ 470 MHz										
Antenna Location	Antenna	Gain (dBi)	Meas. Distance (cm)	E/H Field	Calibration Factor	Average over Head, Chest, Lower Trunk Back/Front seats (mW/cm^2)		Initial Power (W)	Pwr. Density Calc. (mW/cm^2)	Pwr. Density Max Calc. (mW/cm^2)
						Back	Front			
Roof (cnt)	PMAE4034 A	7.15	Highest Reading	E	1.01	0.060	0.038	44.6	0.030	0.03
Measurement Grid										
Test Position	% of Control Limit Head		% of Control Limit Chest		% of Control Limit Lower Trunk		IEEE Controlled Limit:		1.57	
Back Seat	3.7%		3.4%		4.3%		IEEE Uncontrolled Limit:		0.31	
Front Seat	1.6%		1.8%		3.9%		RF Po (*Max):		48.0	



COMPUTATIONAL EME COMPLIANCE ASSESSMENT OF THE XPR UHF MOBILE RADIO, MODEL # PMUE2345A, FCC ID ABZ99FT4080

November 29, 2006

Giorgi Bit-Babik and Antonio Faraone

Motorola Corporate EME Research Lab, Plantation, Florida

Introduction

This report summarizes the computational [numerical modeling] analysis performed to document compliance of the XPR UHF, Model Number PMUE2345A, Mobile Radio and vehicle-mounted antennas with the Federal Communications Commission (FCC) guidelines for human exposure to radio frequency (RF) emissions. The radio operates in the 403 - 470 MHz frequency band.

This computational analysis supplements the measurements conducted to evaluate the FCC *maximum permissible exposure* (MPE) limits for this mobile device. The test conditions (9 in total) that did not conform with applicable MPE limits were analyzed to determine whether those conditions complied with the *specific absorption rate* (SAR) limits for general public exposure (1.6 W/kg averaged over 1 gram of tissue and 0.08 W/kg averaged over the whole body) set forth in FCC guidelines, which are based on the IEEE C95.1-1999 standard [1]. In total 18 independent simulations have been performed which address the exposure to UHF mobile radios with trunk-mount antennas. For all simulations a commercial code based on Finite-Difference-Time-Domain (FDTD) methodology was employed to carry out the computational analysis. It is well established and recognized within the scientific community that SAR is the primary dosimetric quantity used to evaluate the human body's absorption of RF energy and that MPEs are in fact derived from SAR. Accordingly, the SAR computations provide a scientifically valid and more relevant estimate of human exposure to RF energy.

Method

The simulation code employed is XFDTD™ v6.3, by Remcom Inc., State College, PA. This computational suite features a heterogeneous full body standing model (High Fidelity Body Mesh), derived from the so-called Visible Human [2], discretized in 5 mm voxels. The dielectric properties of 23 body tissues are automatically assigned by XFDTD™ at any specific frequency. The “seated” man model was obtained from the standing model by modifying the articulation angles at the hips and the knees. Details of the computational method and model are provided in the Appendix to this report, following the structure outlined in Appendix B.III of the Supplement C to the FCC OET Bulletin 65.

The car model has been imported into XFDTD™ from the CAD file of a sedan car having dimensions 4.98 m (L) x 1.85 m (W) x 1.18 m (H), and discretized in 5mm voxels. For the car model the wheels and part of the hood were omitted in order to fit within the computational memory available. These omissions would not be expected to affect the exposure calculations in any event.

For passenger exposure from mobile radio UHF trunk-mount antennas the distance of antennas from the passenger head was set at 85 cm and the antenna was located at 26 cm distance from the end of the trunk, so as to replicate the experimental conditions used in MPE measurements. Figures 1 shows one of the XFDTD™ computational models used for passenger exposure to trunk mounted antenna.

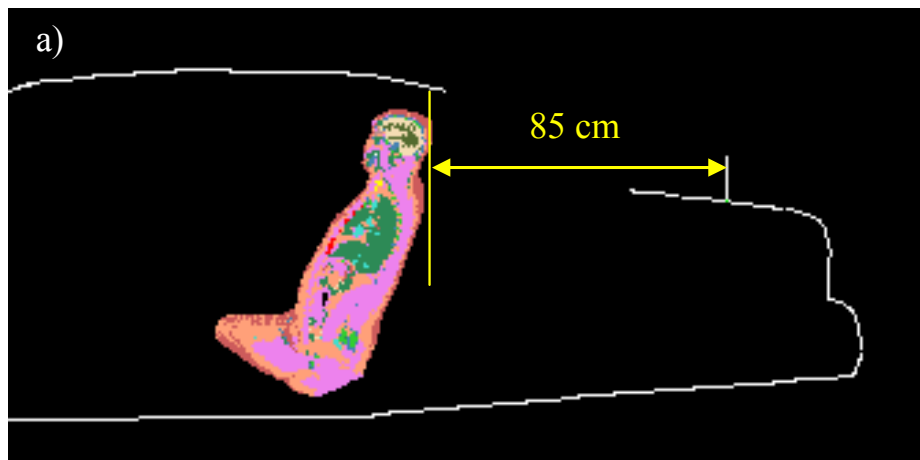




Figure 1: Passenger model exposed to a trunk-mount antenna (34 cm) operating at 470 MHz: XFDTD geometry (a) and H-field distribution (b). The antenna is mounted at 85 cm from the passenger.

The computational code employs a time-harmonic excitation to produce a steady state electromagnetic field in the exposed body. Subsequently, the corresponding SAR distribution is automatically processed in order to determine the whole-body and 1-g average SAR. The maximum output power from UHF mobile radio antenna is 48 W *rms*. Since the ohmic losses in the cable and in the car materials, as well as the mismatch losses at the antenna feed-point, are neglected, and source-based time averaging (50% talk time) is employed, all computational results are normalized to half of it, i.e., 24 W *rms* net output power.

Results of SAR computations for car passengers

The test condition requiring SAR computations is summarized in Table I, together with the antenna data and the SAR results. The condition is for antenna mounted on the trunk. The passenger is located in the center or on the side of the rear seat. The passenger model is surrounded by air, as the seat, which is made out of poorly conductive fabrics, is not included in the computational model. All the transmit frequency, antenna length, and passenger location combinations reported in Table I have been simulated individually. The maximum peak 1-g SAR is 0.251 W/kg, while the maximum whole-body average SAR is 0.00884 W/kg.

Table I: Results of the SAR computations for passenger exposure (50% talk-time).

MPE Table #	Mount location	Antenna Kit #	Antenna length		Freq [MHz]	Exposure location	SAR [W/kg]	
			Physical	XFDTD			1-g	WB
1	Trunk	PMAE4033A	34 cm	35 cm	450	center	0.131	0.00686
2	Trunk	PMAE4033A	34 cm	35 cm	460	center	0.114	0.00697
3	Trunk	PMAE4033A	34 cm	35 cm	470	center	0.172	0.00751
4	Trunk	PMAE4033A	34 cm	35 cm	450	side	0.230	0.00740
5	Trunk	PMAE4033A	34 cm	35 cm	460	side	0.238	0.00808
6	Trunk	PMAE4033A	34 cm	35 cm	470	side	0.251	0.00884
7	Trunk	PMAE4032A	39 cm	40 cm	406	center	0.178	0.00713
8	Trunk	PMAE4032A	39 cm	40 cm	416.5	center	0.211	0.00716
9	Trunk	PMAE4032A	39 cm	40 cm	413	center	0.206	0.00700
10	Trunk	PMAE4032A	39 cm	40 cm	406	side	0.186	0.00716
11	Trunk	PMAE4032A	39 cm	40 cm	416.5	side	0.180	0.00711
12	Trunk	PMAE4032A	39 cm	40 cm	413	side	0.183	0.00708
13	Trunk	PMAE4034A	79 cm	80 cm	450	center	0.063	0.00419
14	Trunk	PMAE4034A	79 cm	80 cm	460	center	0.118	0.00474
15	Trunk	PMAE4034A	79 cm	80 cm	470	center	0.168	0.00584
16	Trunk	PMAE4034A	79 cm	80 cm	450	side	0.217	0.00505
17	Trunk	PMAE4034A	79 cm	80 cm	460	side	0.230	0.00589
18	Trunk	PMAE4034A	79 cm	80 cm	470	side	0.247	0.00702

The SAR distribution in the passenger model in the exposure condition that gave highest 1-g SAR is reported in Fig. 2 (470 MHz, passenger in the side of the back seat, PMAE4033A antenna). The same condition produced highest whole body average SAR.

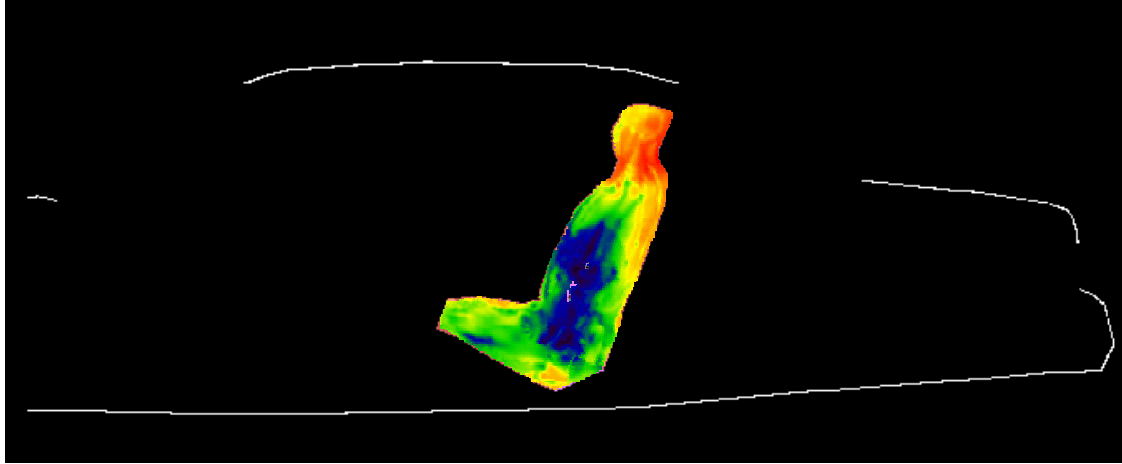


Figure 2. SAR distribution at 470 MHz in the passenger located in the side of the back seat, produced by the trunk-mount PMAE4033A antenna (34 cm). The contour plot in the figure is relative to the plane where the peak 1-g average SAR for this exposure condition occurs.

An example of SAR and H field distribution at 470 MHz in the passenger located in the center of the back seat, produced by the trunk-mount PMAE4033A antenna is shown in Fig 3.

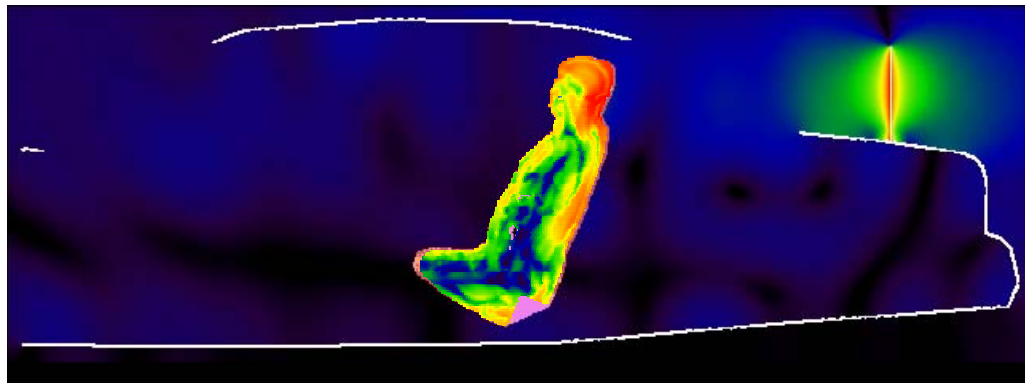


Figure 3. Example of SAR and H field distribution at 470 MHz in the passenger located in the center of the back seat, produced by the trunk-mount PMAE4033A antenna (34 cm).

Another example of SAR and H field distribution at 470 MHz in the passenger located in the center of the back seat, produced by the trunk-mount gain PMAE4034A antenna is shown in Fig 4.

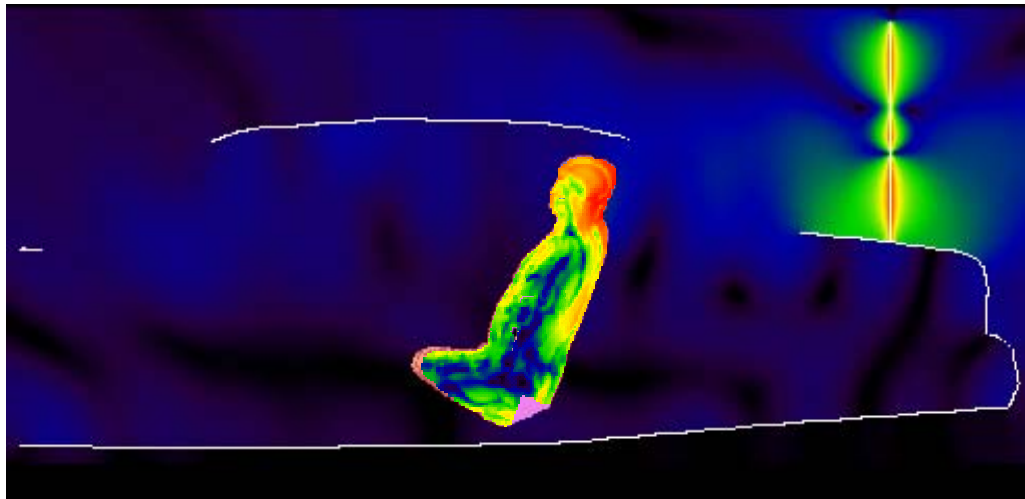


Figure 4. Example of SAR and H field distribution at 470 MHz in the passenger located in the center of the back seat, produced by the trunk-mount PMAE4034A antenna (79 cm).

The last example of SAR and H field distribution at 416.5 MHz in the passenger located in the center of the back seat, produced by the trunk-mount gain PMAE4032A antenna is shown in Fig 5.

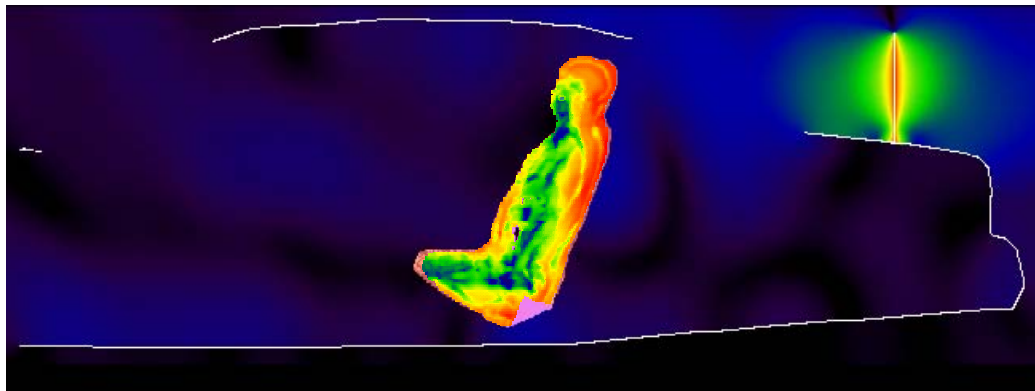


Figure 5. Example of SAR and H field distribution at 416.5 MHz in the passenger located in the center of the back seat, produced by the trunk-mount PMAE4032A antenna (39 cm).

Conclusions

Under the test conditions described for evaluating passenger exposure to the RF electromagnetic fields emitted by vehicle-mounted antennas used in conjunction with this mobile radio product, the present analysis shows that the computed SAR values are compliant with the FCC exposure limits for the general public.

References

- [1] IEEE Standard C95.1-1999. *IEEE Standard for Safety Levels with Respect to Human Exposure to RF Electromagnetic Fields, 3 kHz to 300 GHz.*
- [2] http://www.nlm.nih.gov/research/visible/visible_human.html

APPENDIX: SPECIFIC INFORMATION FOR SAR COMPUTATIONS

This appendix follows the structure outlined in Appendix B.III of the Supplement C to the FCC OET Bulletin 65. Most of the information regarding the code employed to perform the numerical computations has been adapted from the XFDTD™ v5.3 and v6.3 User Manuals. Remcom Inc., owner of XFDTD™, is kindly acknowledged for the help provided.

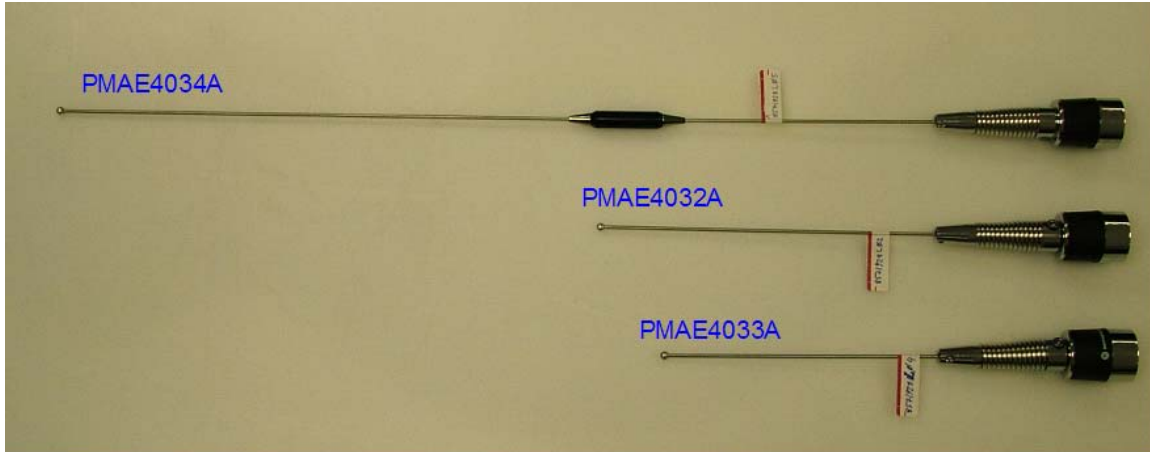
1) Computational resources

- a) A distributed Linux based multi-CPU computer cluster equipped with AMD 64-bit Opteron processors was employed for all simulations.
- b) The memory requirement was close to 3 GB in all cases. Using the above-mentioned system with four processors operating concurrently, the typical simulation would run for 2 hours.

2) FDTD algorithm implementation and validation

- a) We employed a commercial code (XFDTD™ v6.3, by Remcom Inc.) that implements the Yee's FDTD formulation [1]. The solution domain was discretized according to a rectangular grid with a uniform 5 mm step in all directions. Sub-gridding was not used. Liao's absorbing boundary conditions [2] are set at the domain boundary to simulate free space radiation processes. The excitation is a lumped voltage generator with 50-ohm source impedance. The code allows selecting *wire objects* without specifying their radius. We used a wire to represent the antenna. The car body is modeled by solid metal. We did not employ the “thin wire” algorithm in XFDTD™ since the antenna radius was never smaller than one-fifth the voxel dimension. In fact, the XFDTD™ manual specifies that “Thin Wire materials may be used in special situations where a wire with a radius much smaller than the cell size is required... in cases where the wire radius is important to the calculation and is less than approximately 1/5 the cell size, the thin wire material may be used to accurately simulate the correct wire dimensions.” The voxel size in all our simulations was 5 mm, and the antenna radius is always at least 1 mm (1 mm for the short quarter-wave antennas and 1.5 mm for the long gain antennas), so there was no need to specify a “thin wire” material. Because the field impinges on the bystander or passenger model at a distance of several tens of voxels from the antenna, the details of antenna wire modeling are not expected to have significant impact on the exposure level.

Pictures of the antennas PMAE4032A, PMAE4033A, and PMAE4034A are presented below

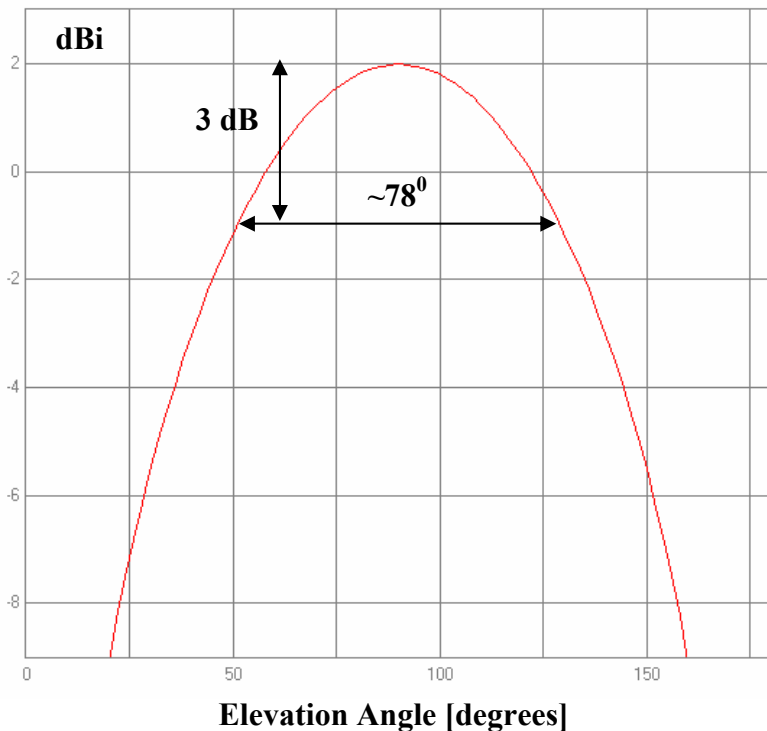
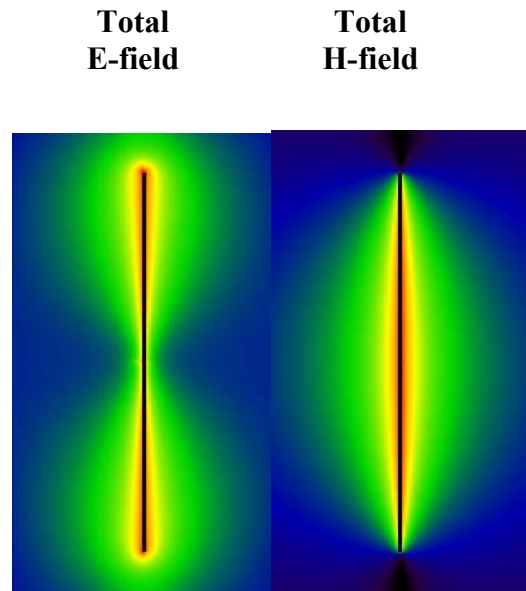


The X-ray of the reactive load in the center of the PMAE4034A antenna is also presented in the next picture below. The reactive load is significantly shorter than the length of the antenna and is less than 1/20 of the wavelength at center operating frequency. It was modeled in XFDTD as lumped reactive element.

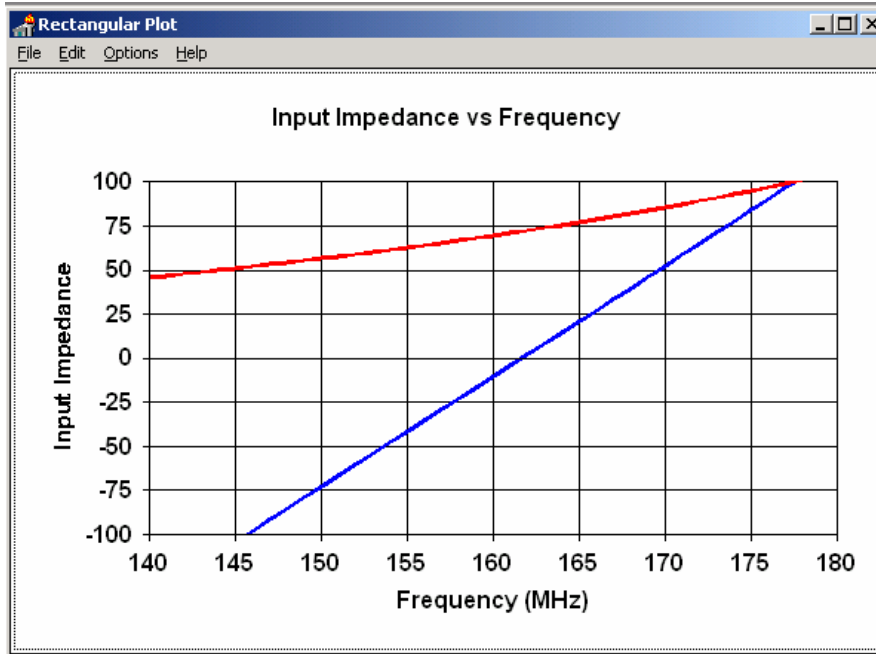


b) XFDTD™ is one of the most widely employed commercial codes for electromagnetic simulations. It has gone through extensive validation and has proven its accuracy over time in many different applications. One example is provided in [3].

We carried out a validation of the code algorithm by running the canonical test case involving a half-wave wire dipole. The dipole is 0.475 times the free space wavelength at 160 MHz, i.e., 88.5 cm long. The discretization used in the model was uniform in all directions and equal to 5 mm, so the dipole was 177 cells long. Also in this case, the “thin wire” model was not needed. The following picture shows XFDTD™ outputs regarding the antenna feed-point impedance ($72.6 - j 11.6$ ohm), as well as qualitative distributions of the total E and H fields near the dipole. The radiation pattern is shown as well (one lobe in elevation). As expected, the 3 dB beamwidth is about 78 degrees.



We also compared the XFDTD™ result with the results derived from NEC [4], which is a code based on the method of moments. In this case, we used a dipole with radius 1 mm, length 88.5 cm, and the discretization is 5 mm. The corresponding input impedance at 160 MHz is $69.5-j10.5$ ohm. Its frequency dependence is reported in the following figure.



This validation ensures that the input impedance calculation is carried out correctly in XFDTD™, thereby enabling accurate estimates of the radiated power. It further ensures that the wire model employed in XFDTD™, which we used to model the antennas, produces physically meaningful current and fields distributions. Both these aspects ensure that the field quantities are correctly computed both in terms of absolute amplitude and relative distribution.

3) Computational parameters

a) The following table reports the main parameters of the FDTD model employed to perform our computational analysis:

PARAMETER	X	Y	Z
Voxel size	5 mm	5 mm	5 mm
Maximum domain dimensions employed for passenger computations with the trunk-mount antennas	387	737	326
Time step	Exactly equal to Courant limit (typically 10 μ s at this frequency, with the body model)		
Objects separation from FDTD boundary (voxels)	>10	>10	>10
Number of time steps for passenger	At least 3000 in all simulations		
Excitation	Sinusoidal (approx 10-12 periods)		

b) In order to fit the model within a grid size that would not use up the available memory, we chopped the hood of the car and the feet of the human model.

4) Phantom model implementation and validation

a) The FDTD mesh of a male human body was created using digitized data in the form of transverse color images. The data is from the *visible human project* sponsored by the National Library of Medicine (NLM) and is available via the Internet (http://www.nlm.nih.gov/research/visible/visible_human.html). The male data set consists of MRI, CT and anatomical images. Axial MRI images of the head and neck and longitudinal sections of the rest of the body are available at 4 mm intervals. The MRI images have 256 pixel by 256 pixel resolution. Each pixel has 12 bits of gray tone resolution. The CT data consists of axial CT scans of the entire body taken at 1 mm intervals at a resolution of 512 pixels by 512 pixels where each pixel is made up of 12 bits of gray tone. The axial anatomical images are 2048 pixels by 1216 pixels where each pixel is defined by 24 bits of color. The anatomical cross sections are also at 1 mm intervals and coincide with the CT axial images. There are 1871 cross sections. The XFDTD™ High Fidelity Body Mesh uses 5x5x5 mm cells and has dimensions 136 x 87 x 397. Dr. Michael Smith and Dr. Chris Collins of the Milton S. Hershey Medical Center, Hershey, Pa, created the High Fidelity Body mesh. Details of body model creation are given in the *methods* section in [5]. The body mesh contains 23 tissues materials. Measured values for the tissue parameters for a broad frequency range are included with the mesh data. The correct values are interpolated from the table of measured data and entered into the appropriate mesh variables. The tissue conductivity and permittivity variation *vs.* frequency is included in the XFDTD™ calculation by a multiple-pole approximation to the Cole-Cole approximated tissue parameters reported by Camelia Gabriel, Ph.D., and Sami Gabriel, M. Sc. (<http://www.brooks.af.mil/AFRL/HED/hedr/reports/dielectric/home.html>).

- a) The XFDTD™ High Fidelity Body Mesh model correctly represents the anatomical structure and the dielectric properties of body tissues, so it is appropriate for determining the highest exposure expected for normal device operation.
- b) One example of the accuracy of XFDTD™ for computing SAR has been provided in [6]. The study reported in [6] is relative to a large-scale benchmark of measurement and computational tools carried out within the IEEE Standards Coordinating Committee 34, Sub-Committee 2.

5) Tissue dielectric parameters

- a) The following table reports the dielectric properties used by XFDTD™ for the 23 body tissue materials in the High Fidelity Body Mesh at 450 MHz.

#	Tissue	ϵ_r	σ (S/m)	Density (kg/m ³)
1	skin	41.5	0.57	1125
2	tendon, pancreas, prostate, aorta, liver, other	50.3	0.76	1151
3	fat, yellow marrow	5.02	0.05	943
4	cortical bone	13.4	0.11	1850
5	cancellous bone	21.0	0.23	1080
6	blood	57.2	1.72	1057
7	muscle, heart, spleen, colon, tongue	63.5	0.99	1059

8	gray matter, cerebellum	54.1	0.88	1035.5
9	white matter	39.7	0.54	1027.4
10	CSF	68.9	2.32	1000
11	sclera/cornea	54.4	1.04	1151
12	vitreous humor	68.3	1.56	1000
13	bladder	17.6	0.31	1132
14	nerve	35.5	0.50	1112
15	cartilage	43.4	0.66	1171
16	gall bladder bile	76.5	1.62	928
17	thyroid	59.8	0.82	1035.5
18	stomach/esophagus	74.4	1.13	1126
19	lung	52.8	0.72	563
20	kidney	57.0	1.16	1147
21	testis	65.2	1.13	1158
22	lens	51.9	0.71	1163
23	small intestine	73.7	2.07	1153

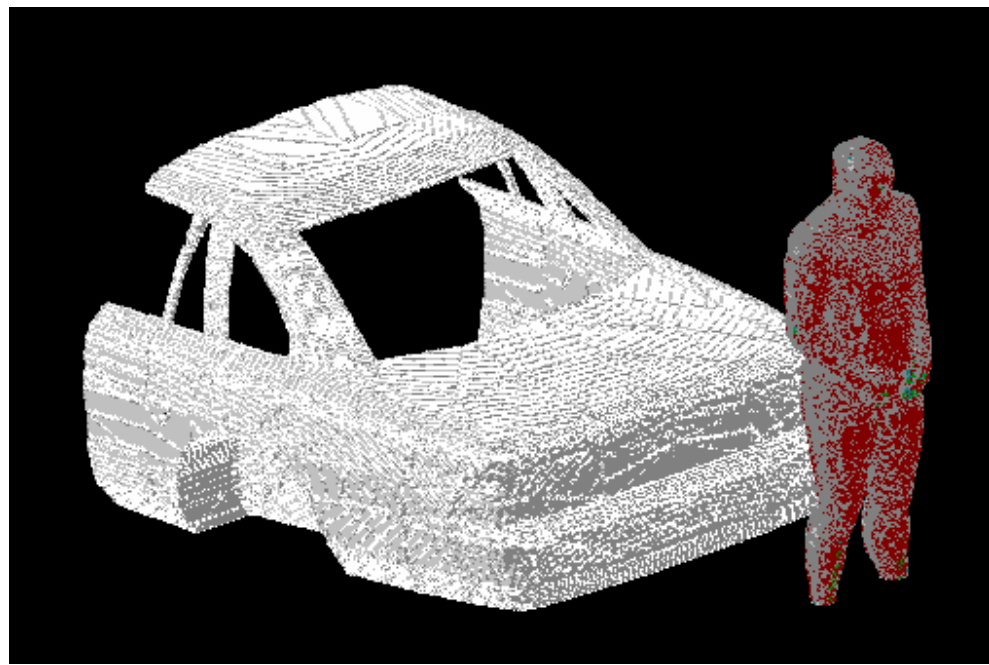
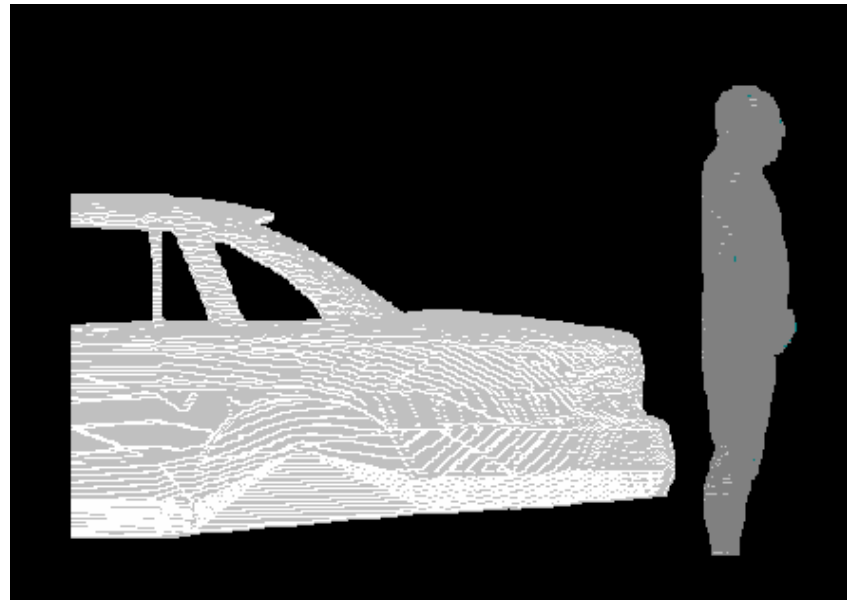
b) The tissue types and dielectric parameters used in the SAR computation are appropriate for determining the highest exposure expected for normal device operation, because they are derived from measurements performed on real biological tissues (<http://www.brooks.af.mil/AFRL/HED/hedr/reports/dielectric/home.html>).

c) The tabulated list of the dielectric parameters used in phantom models is provided at point 5(a). As regards the device (car plus antenna), we used perfect electric conductors.

6) Transmitter model implementation and validation

a) The essential features that must be modeled correctly for the particular test device model to be valid are:

- Car body. We developed one very similar to the car used for MPE measurements, so as to be able to correlate measured and simulated field values. The model was imported in XFDTD™ from a CAD model that is commercially available at <http://www.3dcadbrowser.com/>
- Antenna. We used a straight wire in all cases, even though the gain antenna has a base coil for tuning. All the coil does is compensating for excess capacitance due to the antenna being slightly longer than half a wavelength. We do not need to do that in the model, as we used normalization with respect to the net radiated power, which is determined by the input resistance only. In this way, we neglect mismatch losses and artificially produce an overestimation of the SAR, thereby introducing a conservative bias in the model.
- Antenna location. We used the same location, relative to the edge of the car trunk, the backseat, or the roof, used in the MPE measurements. The following pictures show a lateral and a perspective view of the whole model (XFDTD™ does not show wires in this type of view, that is why the antenna is not visible).



The car model is constituted by perfect electric conductor and does not include wheels in order to reduce its complexity. The passenger model is surrounded by air, as the seat, which is made out of poorly conductive fabrics, is not included in the computational model. The pavement has not been included in the model.

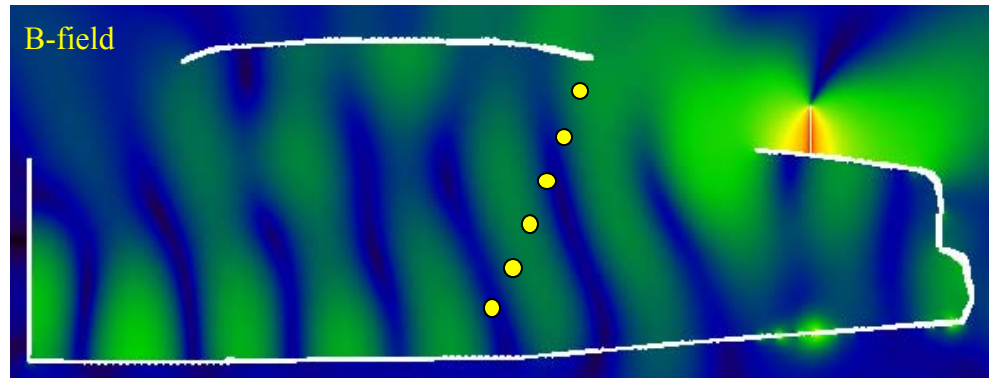
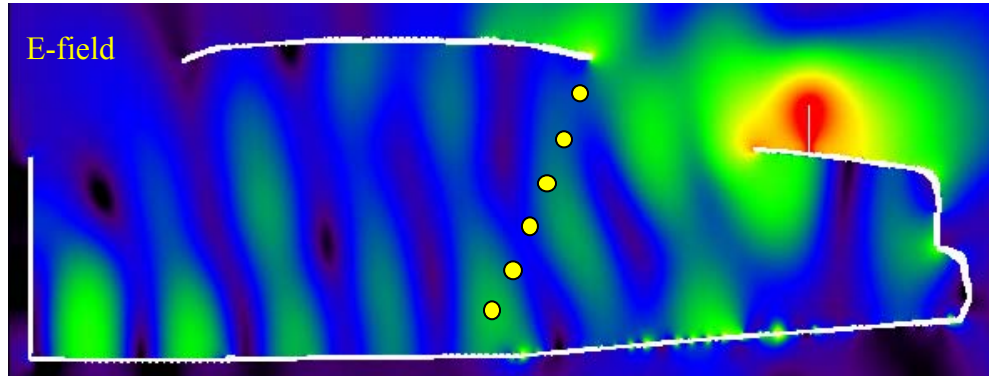
The passenger and bystander models were validated for similar antenna and frequency conditions by comparing the MPE measurements at two UHF frequencies (421.5 MHz and 425 MHz). The validation at 421.5 MHz was performed in 2004 (FCC ID#ABZ99FT4064). The corresponding MPE measurements are reported in the compliance report relative to FCC ID#ABZ99FT4064. The comparison results are

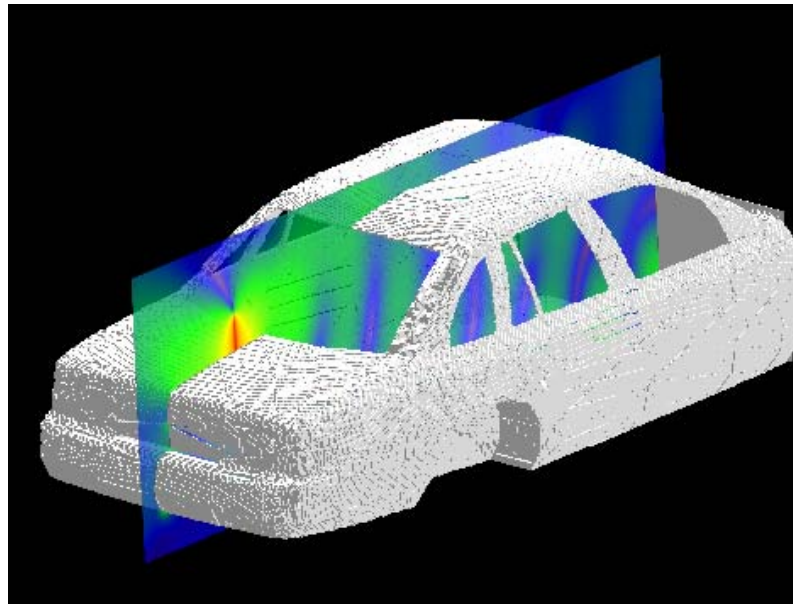
presented below, according to following definitions for the equivalent power densities (based on E or H-field):

$$S_E = \frac{|\mathbf{E}|^2}{2\eta}, \quad S_H = \frac{\eta}{2} |\mathbf{H}|^2, \quad \eta = 377 \Omega$$

Passenger with 17.5 cm monopole antenna (HAE4002A 421.5 MHz)

The following figure of the test model shows the car model, where the yellow dots individuate the back seat, as it can be observed from the other figure showing the cross section of the passenger. The comparison has been performed by taking the average of the computed steady-state field values at the six dotted locations, corresponding to the head, chest, and legs along the yellow dots line, and comparing them with the average of the MPE measurements performed at the head, chest and legs locations. Such a comparison is carried out at the same rms power level (22 W, including the 50% duty factor) used in the MPE measurements.





The equivalent power density (S) is computed from the E-field and the H-field separately. The following table reports the E-field values computed by XFDTD™ at the six locations, and the corresponding power density.

Location Number	E-field, V/m	Eq. Power Density 1.0 V source	Scaled Power Dens. 22 W output, mW/cm^2
1	5.83E-01	4.51E-04	4.41E-01
2	6.31E-01	5.28E-04	5.16E-01
3	6.50E-01	5.60E-04	5.48E-01
4	5.50E-01	4.01E-04	3.92E-01
5	4.50E-01	2.69E-04	2.63E-01
6	7.80E-01	8.07E-04	7.89E-01
Equivalent average Power Density			4.92E-01

Location Number	B-field, Weber/m ²	Eq. Power Density 1.0 V source	Scaled Power Dens. 22 W output, mW/cm ²
1	2.26E-09	0.00061	5.96E-01
2	9.00E-10	0.00010	9.45E-02
3	1.20E-09	0.00017	1.68E-01
4	2.20E-09	0.00058	5.65E-01
5	1.90E-09	0.00043	4.21E-01
6	9.00E-10	0.00010	9.45E-02
Equivalent average Power Density			3.23E-01

The input impedance is $36.2+j24.8$ ohm, therefore the radiated power (considering the mismatch to the 50 ohm unitary voltage source) is 2.25E-3 W, therefore a factor equal to 9779 is required to scale up to 22 W radiated. The corresponding scaled-up power densities are reported in the tables above, which show that the simulation overestimates the average power density from the MPE measurements (0.29 mW/cm^2), as derived from the measured E-field reported in the following table:

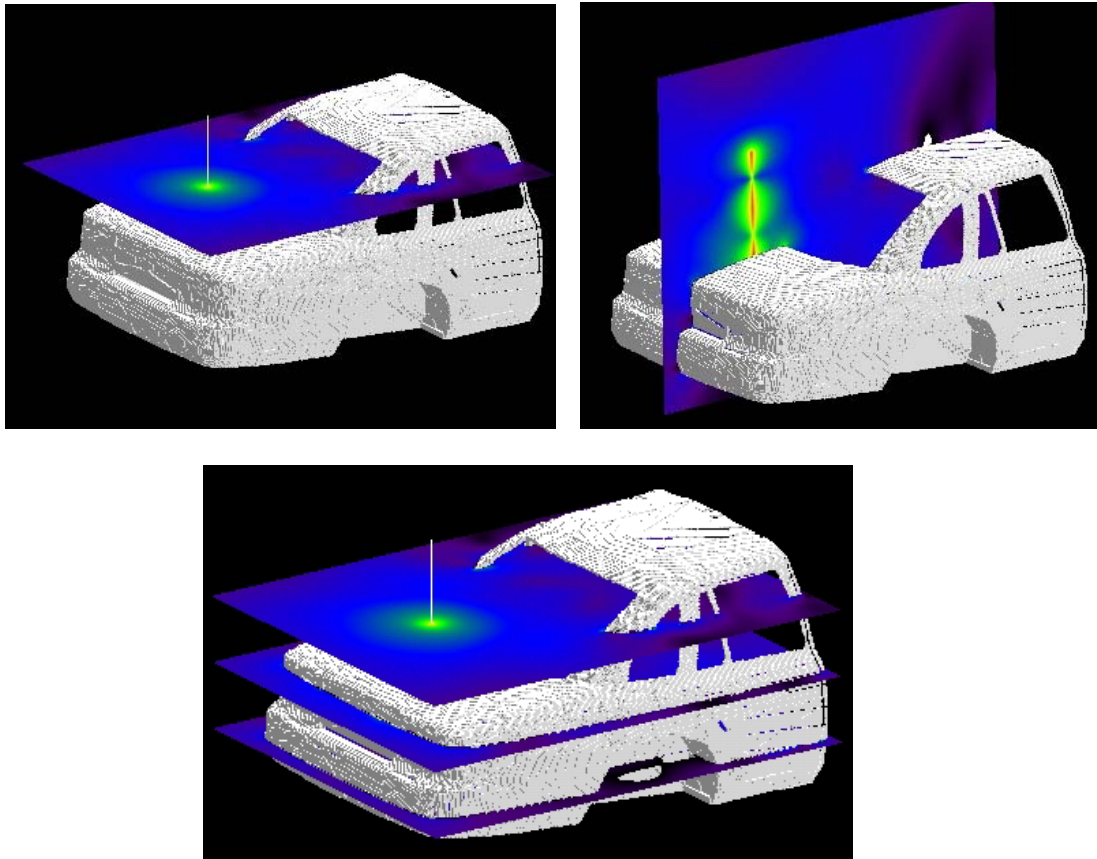
Position	SE (meas), 22 W output mW/cm ²
Head	0.38
Chest	0.33
Lower Trunk	0.16

The simulations tend to overestimate the average power density levels, which is understandable since there are no ohmic losses and perfect impedance matching is enforced in the computational models. Based on these results, we conclude that the simulation will produce slight exposure overestimates (about 12%).

- b) Descriptions and illustrations showing the correspondence between the modeled test device and the actual device, with respect to shape, size, dimensions and near-field radiating characteristics, are found in the main report.
- c) Verification that the test device model is equivalent to the actual device for predicting the SAR distributions descends from the fact that the car and antenna size and location in the numerical model correspond to those used in the measurements.
- d) The peak SAR is in the neck region for the passenger, which is in line with MPE measurements and predictions.

Passenger with 63.5 cm monopole antenna (HAE6010A 425 MHz)

The following figures show the car model with the field distribution in the horizontal planes where the MPE measurements have been performed. The comparison has been performed by taking the average of the computed steady-state field values at the three locations, corresponding to the head, chest, and lower trunk, and comparing them with the average of the MPE measurements performed at the head, chest and lower trunk locations. Such a comparison is carried out at the same rms power level (61.5 W, including the 50% duty factor) used in the MPE measurements.



The equivalent power density (S) is computed from the E-field. The following table reports the E-field values computed by XFDTD™ at the three locations, and the corresponding power density.

Location Number	E-field, V/m	Eq. Power Density 1.0 V source	Scaled Power Dens. 61.5 W output, mW/cm^2
1	2.10E-01	5.85E-05	0.561
2	3.66E-01	1.78E-04	1.70
3	1.72E-01	3.92E-04	0.376
Equivalent average Power Density			0.88

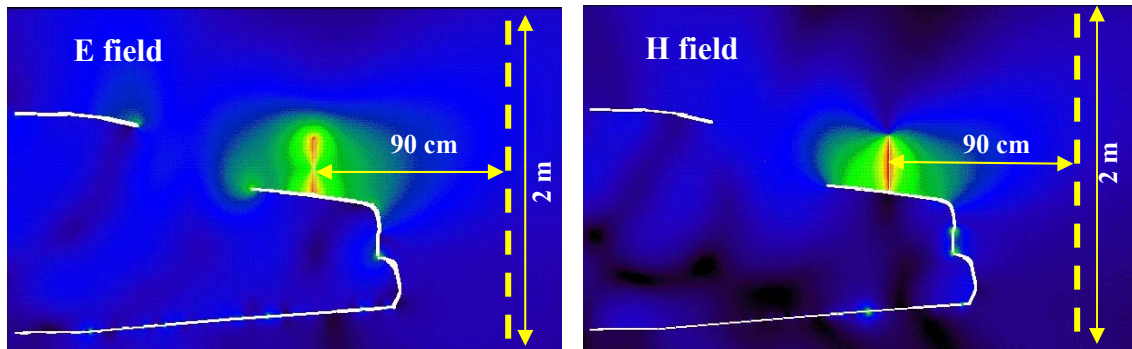
The corresponding scaled-up power densities are reported in the tables above, which show that the simulation overestimates the average power density from the MPE measurements (0.52 mW/cm^2), as derived from the measured E-field reported in the following table:

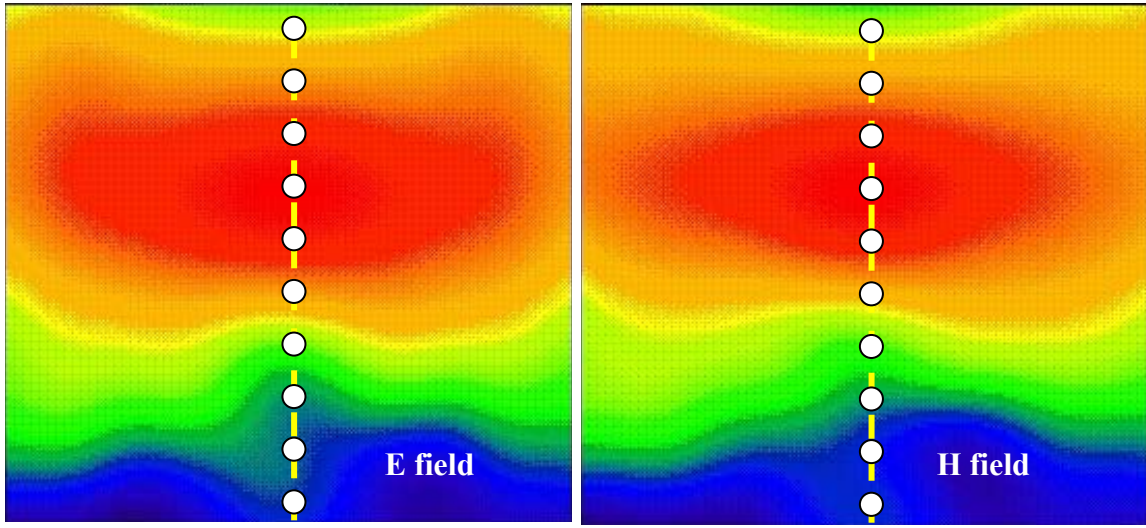
Position	SE (meas), 60 W output mW/cm^2
Head	0.72
Chest	0.64
Lower Trunk	0.19

The simulations tend to overestimate the average power density levels, which is understandable since there are no ohmic losses and perfect impedance matching is enforced in the computational models. Based on these results, we conclude that the simulation will produce exposure overestimates (about 69%).

Bystander with 29 cm monopole antenna (HAE6013A 425 MHz)

The following figures show the E-field and H-field distributions across a vertical plane passing for the antenna and cutting the car in half. As done in the measurements, the MPE is computed from both E-field and H-field distributions, along the yellow dotted line at 10 points spaced 20 cm apart from each other up to 2 m in height. These lines and the field evaluation points are approximately indicated in the figures. The E-field and H-field distributions in the vertical plane placed at 90 cm from the antenna, behind the case, are shown as well. The points where the fields are sampled to determine the equivalent power density (S) are approximately indicated by the white dots. A picture of the antenna is not reported because it is identical to the HAE6013A.

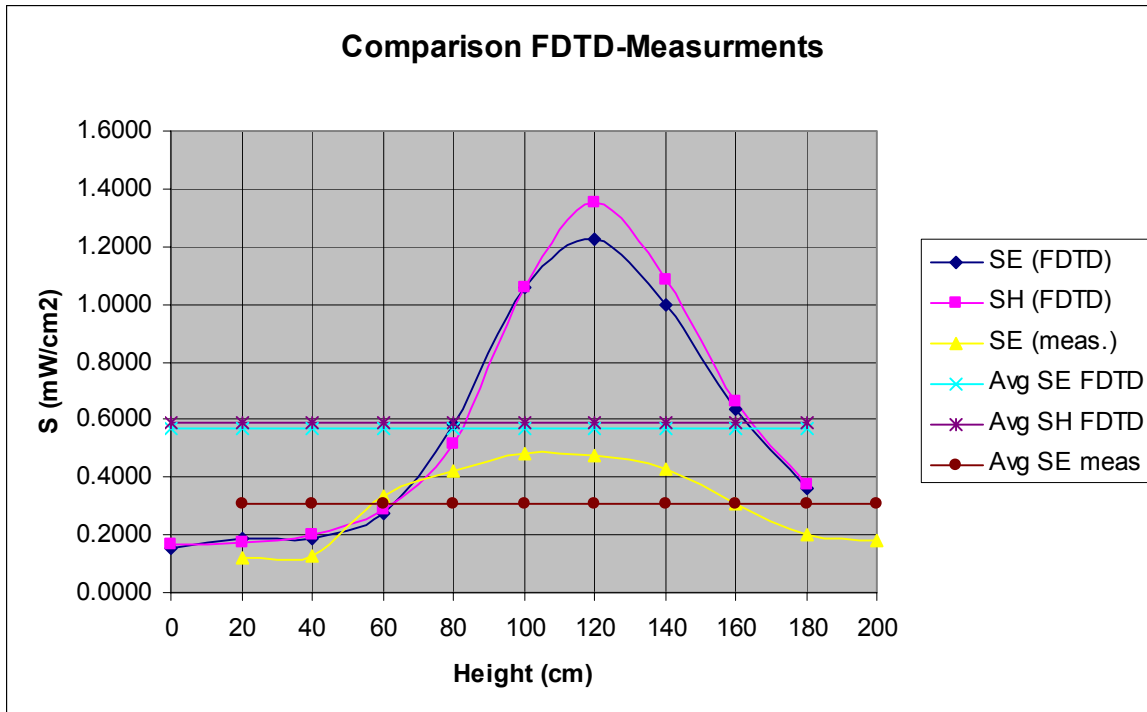




The following table reports the field values computed by XFDTD™ and the corresponding power density values. The average exposure levels are computed as well.

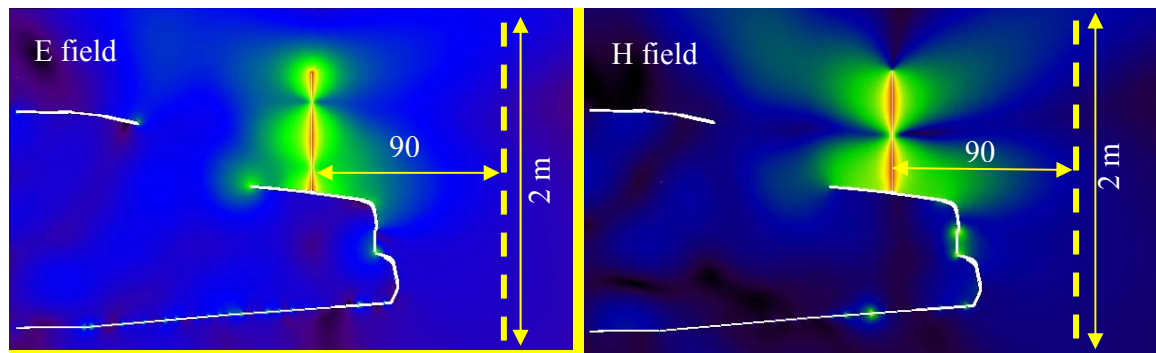
Height (cm)	E (V/m)	S_E (W/m ²)	H (A/m)	S_H (W/m ²)
0	1.05E-01	1.46E-05	2.90E-05	1.589E-05
20	1.14E-01	1.72E-05	2.90E-05	1.598E-05
40	1.16E-01	1.78E-05	3.14E-05	1.871E-05
60	1.39E-01	2.56E-05	3.75E-05	2.669E-05
80	2.03E-01	5.47E-05	5.03E-05	4.795E-05
100	2.73E-01	9.88E-05	7.23E-05	9.923E-05
120	2.94E-01	1.15E-04	8.17E-05	1.266E-04
140	2.65E-01	9.31E-05	7.32E-05	1.016E-04
160	2.12E-01	5.96E-05	5.73E-05	6.219E-05
180	1.60E-01	3.40E-05	4.32E-05	3.531E-05
Average S_E		5.302E-05	Average S_H	

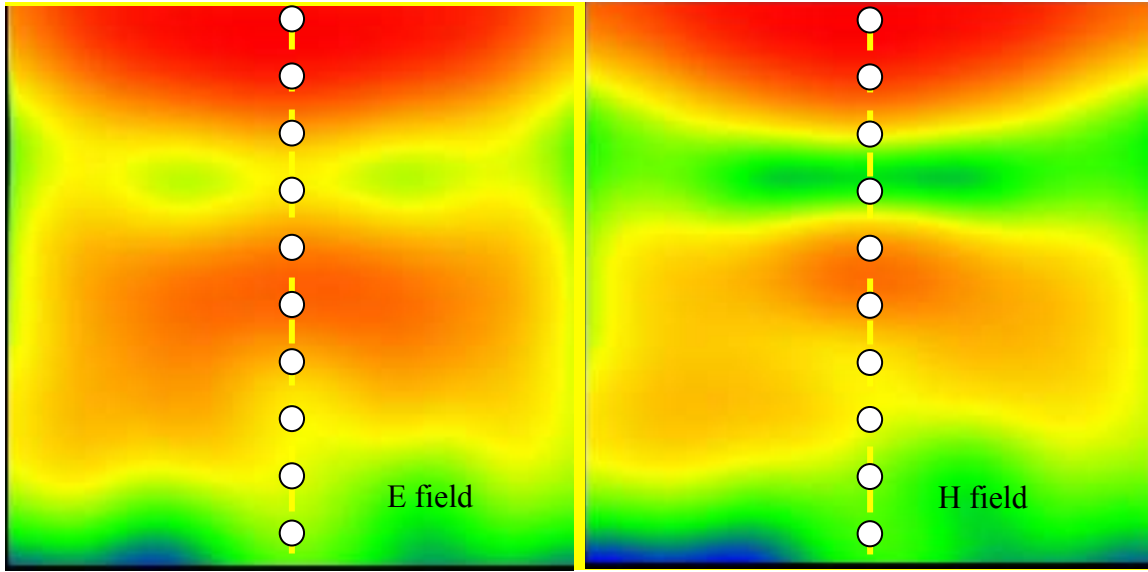
Since the conducted power during the MPE measurement was 123 W the calculated power density was then scaled up for 61.5 W radiated power (taking into account 50% talk time). This model does not include the mismatch loss, loss in the cable and finite conductivity of the car surface and as represents a conservative model for exposure assessment. The scaled-up power density values for 61.5 W radiated power are 5.67 W/m² (E), and 5.88 W/m² (H), that correspond to 0.57 mW/cm² (E), and 0.59 mW/cm² (H). Measurements yielded average power density of 0.309 mW/cm² (E), which shows that the calculated power density is overestimated. The following graph shows a comparison between the measured power density and the simulated one, based on E or H fields, normalized to 61.5 W radiated power.



Bystander with 63.5 cm monopole antenna (HAE6010A 425 MHz)

The following figures show the E-field and H-field distributions across a vertical plane passing for the antenna and cutting the car in half. As done in the measurements, the MPE is computed from both E-field and H-field distributions, along the yellow dotted line at 10 points spaced 20 cm apart from each other up to 2 m in height. These lines and the field evaluation points are approximately indicated in the figures. The E-field and H-field distributions in the vertical plane placed at 90 cm from the antenna, behind the case, are shown as well. The points where the fields are sampled to determine the equivalent power density (S) are approximately indicated by the white dots. A picture of the antenna is not reported because it is identical to the HAE6010A.



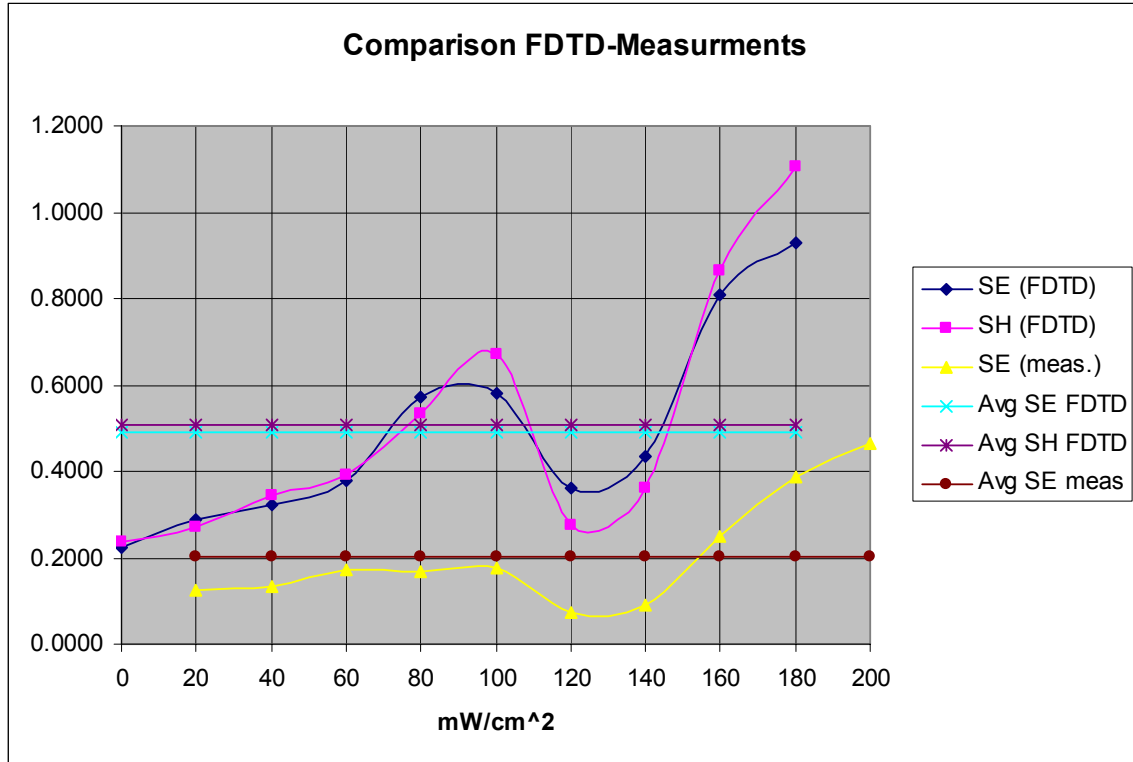


The following table reports the field values computed by XFDTD™ and the corresponding power density values. The average exposure levels are computed as well.

Height (cm)	E (V/m)	S_E (W/m ²)	H (A/m)	S_H (W/m ²)
0	1.32E-01	2.31E-05	4.51E-10	2.43E-05
20	1.49E-01	2.94E-05	4.82E-10	2.77E-05
40	1.58E-01	3.31E-05	5.44E-10	3.53E-05
60	1.71E-01	3.88E-05	5.79E-10	4.00E-05
80	2.10E-01	5.85E-05	6.78E-10	5.48E-05
100	2.12E-01	5.96E-05	7.60E-10	6.89E-05
120	1.67E-01	3.70E-05	4.86E-10	2.82E-05
140	1.83E-01	4.44E-05	5.57E-10	3.70E-05
160	2.50E-01	8.29E-05	8.62E-10	8.86E-05
180	2.68E-01	9.53E-05	9.75E-10	1.13E-04
Average S_E		5.38E-05	Average S_H	

Since the conducted power during the MPE measurement was 123 W the calculated power density was then scaled up for 61.5 W radiated power (taking into account 50% talk time). This model does not include the mismatch loss, loss in the cable and finite conductivity of the car surface and as represents a conservative model for exposure assessment. The scaled-up power density values for 61.5 W radiated power are 5.25 W/m² (E), and 5.06 W/m² (H), that correspond to 0.52 mW/cm² (E), and 0.51 mW/cm² (H). Measurements yielded average power density of 0.204 mW/cm² (E), which shows that the calculated power density is overestimated. The following graph shows a comparison between the measured power density and the simulated one, based on E or H

fields, normalized to 61.5 W radiated power.



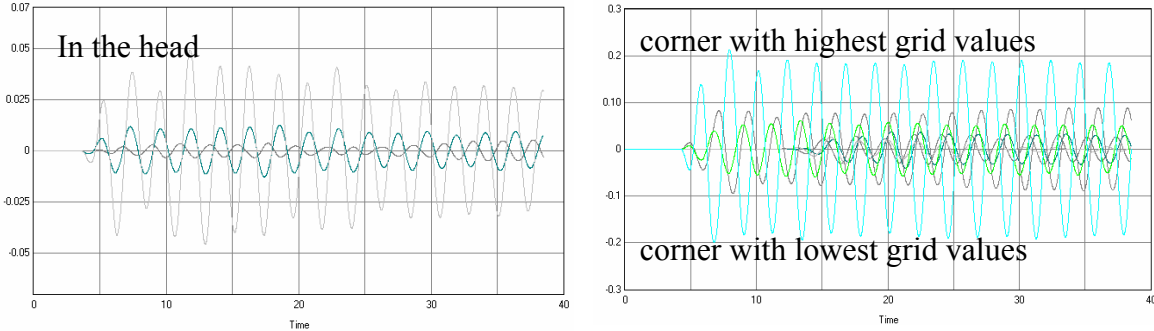
7) Test device positioning

- a) A description of the device test positions used in the SAR computations is provided in the SAR report.
- b) Illustrations showing the separation distances between the test device and the phantom for the tested configurations are provided in the SAR report.

8) Steady state termination procedures

- a) The criteria used to determine that sinusoidal steady-state conditions have been reached throughout the computational domain for terminating the computations are based on the monitoring of field points to make sure they converge. For at least one passenger and one bystander exposure condition, we placed one “field sensor” near the antenna, others between the body and the domain boundary at different locations, and one inside the head of the model. In all simulations, isotropic E-field sensors were placed at opposite corners of the computational domain. We used isotropic E and H field “sensors”, meaning that all three components of the fields are monitored at these points. The

following figures show an example of the time waveforms at the field point sensors in the head and in two opposite points in the computational domain. In the latter case, we selected points near the lowest and highest grid index points. They are shown together in the figure. The highest field levels are observed for the higher index point, as it is closer to the antenna. In all cases, the field reaches the steady-state after a few cycles.



b) 4000 time steps were used, with a time step approximately equal to 10 ps (meeting the Courant criterion), which corresponds to 18 wave periods at 450 MHz.

c) The XFDTD™ algorithm determines the field phasors by using the so-called “two-equations two-unknowns” method. Details of the algorithm are explained in [7].

9) Computing peak SAR from field components

- a) The twelve E-field phasors at the edges of each Yee voxel are combined to yield the SAR associated to that voxel. In particular, the average is performed on the SAR values computed at the 12 edges of each voxel. Notice that in XFDTD™ the dielectric tissue properties are assigned to the voxel edges, thereby allowing said averaging procedure.
- b) The IEEE Standards Coordinating Committee 34, Sub-Committee 2 draft standard P1529 (June 2000) discusses several algorithms for volumetric SAR averaging. It states that “It is observed that while the 12 components algorithm is the most appropriate from the mathematical point of view, the differences in 1g SAR calculated with either the 12 or 6 component methods are negligible for practical mesh resolutions (below 5mm). On the other hand, it is shown that the 3 components approach may lead to significant errors.” XFDTD™ employs the 12-component method, which is the one recommended in the draft standard, thus providing the best achievable accuracy.

10) One-gram averaged SAR procedures

- a) XFDTD™ computes the Specific Absorption Rate (SAR) in each complete cell containing lossy dielectric material and with a non-zero material density. To be considered a complete cell, the twelve cell edges must belong to lossy dielectric materials. The averaging calculation uses an interpolation scheme for finding the averages. Cubical spaces centered on a cell are formed and the mass and average SAR of

the sample cubes are found. The size of the sample cubes increases until the total mass of the enclosed exceeds either 1 or 10 grams. The mass and average SAR value of each cube is saved and used to interpolate the average SAR values at either 1 or 10 grams. The interpolation is performed using two methods (polynomial fit and rational function fit) and the one with the lowest error is chosen. The sample cube must meet some conditions to be considered valid. The cube may contain some non-tissue cells, but some checks are performed on the distribution of the non-tissue cells. A valid cube will not contain an entire side or corner of non-tissue cells.

- b) The sample cube increases in odd-numbered steps (1x1x1, 3x3x3, 5x5x5, etc) to remain centered on the desired cell. Since the visible human model employed herein has 5 mm resolution, the one-gram SAR is computed by averaging first over 1x1x1 voxels, corresponding to 0.125 cm³ (not enough yet), and then over a 3x3x3 voxel cube, corresponding to about 3.4 cm³, which is enough to include 1-g, and finally over a 5x5x5 voxel cube, corresponding to about 15.6 cm³, which includes 10-g. The 1-g average SAR is computed by interpolating these three data points. This procedure is repeated in the surroundings of each voxel that is constituted by lossy materials, so as to determine the 1-g and/or 10-g SAR distributions.
- c) As mentioned at points 10(a) and 10(b), the 1- gram average SAR is determined by interpolating the average SAR for the 1x1x1 , 3x3x3, and the 5x5x5 data points, corresponding to 0.125 cm³, 3.4 cm³, and 15.6 cm³, respectively. Because the interpolation is carried out across three data points, the error introduced should be negligible because the interpolating curve crosses exactly the data points.

11) Total computational uncertainty – We derived an estimate for the uncertainty of FDTD methods in evaluating SAR by referring to [6]. In Fig. 7 in [6] it is shown that the deviation between SAR estimates using the XFDTD™ code and those measured with a compliance system are typically within 10% when the probe is away from the phantom surface so that boundary effects are negligible. In that example, the simulated SAR always exceeds the measured SAR.

As discussed in 6(a), a conservative bias has been introduced in the model so as to reduce concerns regarding the computational uncertainty related to the car modeling, antenna modeling, and phantom modeling. The results of the comparison between measurements and simulations presented in 6(a) suggest that the present model produces an overestimate of the exposure between 4% and 36%. Such a conservative bias should eliminate the need for including uncertainty considerations in the SAR assessment.

12) Test results for determining SAR compliance

- a) Illustrations showing the SAR distribution of dominant peak locations produced by the test transmitter, with respect to the phantom and test device, are provided in the SAR report.
- b) The input impedance and the total power radiated under the impedance match

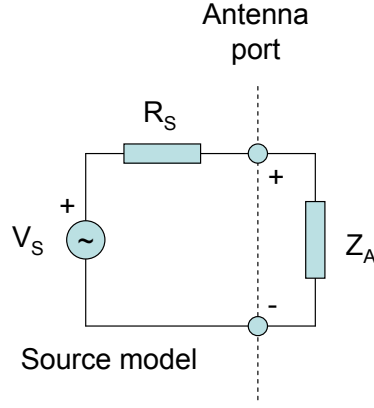
conditions that occur at the test frequency are provided by XFDTD™. XFDTD™ computes the input impedance by following the method outlined in [8], which consists in performing the integration of the steady-state magnetic field around the feed point edge to compute the steady-state feed point current (I), which is then used to divide the feed-gap steady-state voltage (V). The net *rms* radiated power is computed as

$$P_{XFDTD} = \frac{1}{2} \operatorname{Re} \{ VI^* \}$$

Both the input impedance and the net *rms* radiated power are provided by XFDTD™ at the end of each individual simulation.

We normalize the SAR to such a power, thereby obtaining SAR per radiated Watt (*normalized SAR*) values for the whole body and the 1-g SAR. Finally, we multiply such normalized SAR values times the max power rating of the device under test. In this way, we obtain the exposure metrics for 100% talk-time, i.e., without applying source-based time averaging.

A Thevenin model showed in the following figure, featuring a voltage source V_s and real source impedance R_s , is employed in XFDTD to represent the antenna feed.

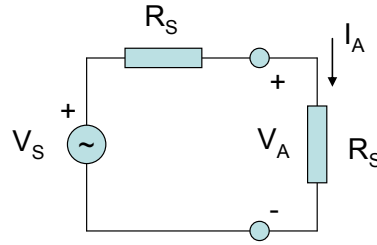


The antenna impedance is $Z_A = R_A + j X_A$. The available power from the source is the one that would be dissipated on the load if perfect the impedance match condition ($Z_A = R_s$) is enforced:

$$P_{av} = \frac{1}{2} \operatorname{Re} \{ V_A I_A^* \} = \frac{1}{2} \frac{V_s}{2} \frac{V_s^*}{2R_s} = \frac{|V_s|^2}{8R_s}.$$

The operative condition under which the available power is measured is represented in the following figure. Note that this is the same condition, where the load resistance is

represented by a power metering device, used to measure the maximum conducted power from a radio.



Therefore, it is possible to establish the Thevenin voltage that would be representative of a radio transmitter with maximum rated power P_{\max} as follows:

$$P_{\max} = \frac{|V_s|^2}{8R_s} \Rightarrow |V_s| = \sqrt{8R_s P_{\max}}.$$

When the transmitter is connected to an antenna that exhibits an input impedance Z_A , the power radiated is less or equal than the maximum rated power because of two physical mechanisms: energy dissipation in the antenna structure and energy reflection at the antenna port. The first mechanism is due to dielectric and ohmic losses while the second one is due to the impedance mismatch at the antenna port. Neglecting energy dissipation is a mean to introduce a conservative bias in the compliance assessments. In XFDTD, this is accomplished by defining ideal (non lossy) material properties for the radiating structures. Additional conservative bias is introduced by neglecting the mismatch losses. The mismatch loss factor is:

$$\eta = \frac{P_{\text{rad}}}{P_{\max}} = 1 - |\Gamma|^2 = 1 - \left| \frac{Z_A - R_s}{Z_A + R_s} \right|^2 = \frac{4R_s Z_A}{(Z_A + R_s)^2},$$

where Γ is the reflection coefficient at the antenna port. Therefore, in order to neglect the mismatch loss, in XFDTD the fields are scaled up by a factor $\sqrt{1/\eta}$. This is equivalent to setting $P_{\text{rad}} = P_{\max}$ and therefore $\Gamma = 0$, which is equivalent to say that there are no mismatch losses and that the maximum rated power of the radio transmitter is radiated.

c) For mobile radios, 50% source-based time averaging is applied by multiplying the SAR values determined at point 12(b) times a 0.5 factor.

REFERENCES

- [1] K. S. Yee, "Numerical Solution of Initial Boundary Value Problems Involving Maxwell's Equations in Isotropic Media," *IEEE Transactions on Antennas and Propagation*, vol. 14, no. 3, 302-307, March 1966.
- [2] Z. P. Liao, H. L. Wong, G. P. Yang, and Y. F. Yuan, "A transmitting boundary for transient wave analysis," Scientia Sinica, vol. 28, no. 10, pp 1063-1076, Oct. 1984.
- [3] Validation exercise: Mie sphere. Remcom Inc. (enclosed PDF)



Remcom.pdf

- [4] NEC-Win PRO TM v 1.1, Nittany Scientific, Inc., Riverton, UT.

- [5] C. M. Collins and M. B. Smith, "Calculations of B1 distribution, SNR, and SAR for a surface coil against an anatomically-accurate human body model," *Magn. Reson. Med.*, 45:692-699, 2001. (enclosed TIF)



Collins & Smith.pdf

- [6] Martin Siegbahn and Christer Törnevik, "Measurements and FDTD Computations of the IEEE SCC 34 Spherical Bowl and Dipole Antenna," Report to the IEEE Standards Coordinating Committee 34, Sub-Committee 2, 1998. (enclosed PDF)



Ericsson.pdf

- [7] C. M. Furse and O. P. Gandhi, "Calculation of electric fields and currents induced in a millimeter-resolution human model at 60 Hz using the FDTD method with a novel time-to-frequency-domain conversion," Antennas and Propagation Society International Symposium, 1996. (enclosed PDF)



Furse & Gandhi.pdf

[8] *The Finite Difference Time Domain Method for Electromagnetics*, Chapter 14.2, by K. S. Kunz and R. J. Luebbers, CRC Press, Boca Raton, Florida, 1993.